U.S.NRC
United States Nuclear Regulatory Commission
Protecting People and the Environment

RIL 2025-03
RCD-25-008-0

Phantom with Moving Arms and Legs (PiMAL) Version 6

Date Published: April 2025

Prepared by:
Z. Tucker
C. Rose
J. Luitjens
D. Hamby

Renaissance Code Development, LLC
310 NW 5th St., Suite 203
Corvallis, Oregon 97330

Brian Allen, NRC Project Manager

Research Information Letter
Office of Nuclear Regulatory Research

Disclaimer

Legally binding regulatory requirements are stated only in laws, NRC regulations, licenses, including technical specifications, or orders; not in Research Information Letters (RILs). A RIL is not regulatory guidance, although NRC's regulatory offices may consider the information in a RIL to determine whether any regulatory actions are warranted.

Phantom with Moving Arms and Legs (PiMAL) Version 6

April 2025

Renaissance Code Development, LLC
310 NW 5th St., Suite 203
Corvallis, Oregon 97330
(541) 286-4428
https://www.rcdsoftware.com

Preparer: Charlotte Rose
DN: cn=Charlotte Rose, o=Renaissance Code Development, ou=Research Scientist, email=charlotte.rose@rcdsoftware.com, c=US
Date: 2025.03.31 08:03:46 -07'00'

Reviewer: David Hamby
DN: cn=David Hamby, o=Renaissance Code Development, ou=Operations Manager, email=david.hamby@rcdsoftware.com, c=US
Date: 2025.03.31 08:05:55 -07'00'

Approver: Jeffrey Luitjens
cn=Jeffrey Luitjens, o=Renaissance Code Development, ou=Director - Software Division, email=jeff.luitjens@rcdsoftware.com, c=US
2025.03.31 08:09:37 -07'00'

ABSTRACT

Computational models of the human anthropomorphic phantom have undergone progressive evolution since initial development more than sixty years ago (Xu 2014). Computational phantoms employed by the Nuclear Regulatory Commission (NRC) were largely based on a model published in 1974, which did not account for select organs (e.g., neck, esophagus) and tissues. This was exacerbated by inaccurate organ placement within the body (e.g., thyroid). Most notably, all the computational phantoms were assumed to be in the vertical-upright position, which continues to be a trend in the development of current computational phantoms. To assess the radiation dose in different configurations when needed, the mathematical phantom had been revised to enable freely moving abilities for arms and legs. The revised phantom is called PiMAL: Phantom with Moving Arms and Legs (Akkurt and Eckerman 2007).

The PiMAL software is intended to be coupled with Monte Carlo N-Particle (MCNP) (Pelowitz et al. 2013) to allow radiation transport simulations for estimating radiation dose to humans. The newest version (6.0) also allows dose assessments to humans from medical sources in moveable phantoms of domestic pets (cats, dogs, and horses). The MCNP code can be run natively from the PiMAL interface, or externally in the MCNP command prompt via the generated MCNP input file. Both internal and external sources can be simulated in PiMAL selecting from a drop-down menu in the user interface. The user can also select an organ in the chosen animal in which radioactive material may be placed. Internal sources are assumed to be uniformly distributed within the selected organ. For external sources, in addition to a point source, the user can select the ICRP's standard external exposure geometries (AP, PA, LLAT, RLAT, ISO). Advanced users of MCNP can add their own simulation characteristics to the PiMAL-generated MNCP input deck prior to running the code.

Table of Contents

List of Figures

List of Tables

ACKNOWLEDGMENTS

This report documents work originally performed by Oak Ridge National Laboratory on the development of the PiMAL/MCNP coupled simulation software (Akkurt and Eckerman 2007) and subsequently revised at the request of the US NRC (Contract No. 31310024C0009). This document is a product of RCD and does not necessarily reflect the views or regulatory position of the NRC.

The authors are indebted to B. Allen, S. Bush-Goddard, R. Flora, J. Tomon, V. Shaffer, M. Saba, and S. Sherbini for their support during development and maintenance of many of the RAMP dosimetry models.

1 INTRODUCTION

The PiMAL software is intended to provide input decks for Monte Carlo N-Particle (MCNP) simulations. These files are based on movable human and animal phantoms and their relationship to each other and to the source of a given radiation emission. By itself, the PiMAL software can be useful for scenario visualization, but when used in combination with MCNP its full power is displayed.

Radiation sources can be external to the phantom(s) or embedded in one or more organs of a given phantom. For example, the effective dose to a human female can be assessed for an exposure to her domestic feline having undergone a radioactive iodine treatment for hyperthyroidism.

In the initial phase of development (Akkurt and Eckerman 2007), the objectives for developing PiMAL were three-fold: (1) update the Medical Internal Radiation Dose (MIRD)-5 mathematical phantom model that was then used by the U.S. Nuclear Regulatory Commission (NRC) staff to improve the assessment of dose for realistic exposure configurations; (2) perform benchmark computations against International Council on Radiological Protection (ICRP)-74 (1996) values and investigate the reasons behind any identified discrepancies, and (3) develop an interface to assist the user (or analyst) in using the updated phantom model in dose assessment activities thus reducing staff time.

Updates were made to the organs and compositions of anthropomorphic phantom models. The revised computational phantom model was adopted for radiation transport codes, notably the Monte Carlo N-Particle (MCNP) code (Pelowitz et al. 2013). Computational results generated were compared against values reported by the ICRP in Publication 74 (1996), with discrepancies identified, rectified, and resolved. Although the original PiMAL phantom was developed as an adult hermaphrodite model, with both male and female gender-specific organs for both genders, the latest revision of PiMAL separates the male and female option in the graphical user interface (GUI) for calculating doses. Finally, a GUI assists the analyst with input preparation and output manipulation. The GUI can be used to visualize the positioning of the arms and legs as the desired posture is achieved to generate the input deck, invoke the computations, and extract the organ dose values from the MCNP output deck. The GUI was operating system independent since the coding was done in Java. A phantom model was included in the GUI, thus enabling visualization of the arms and legs as positioned. Once the user decides on the posture, an MCNP input deck can be generated and the radiation transport simulations using MCNP can be performed through the GUI. Furthermore, the organ dose values can be extracted (from the MCNP output deck), displayed, and exported as an American Standard Code for Information Interchange (ASCII) file.

The PiMAL 6.0 project was undertaken to add the capability of including domestic animals (i.e., cat, dog, horse) to the dosimetry simulations, as well as to update data libraries and

coding efficiencies. With increased use of radioactive materials in the treatment protocol for diseases and ailments in pets, a method was needed to estimate radiation dose to humans (e.g., pet owners) from those sources. PiMAL 6.0 allows the user to place an animal phantom in the same MCNP universe with a human phantom. Radioactive source locations in the animal can then be selected for human exposures. At this stage, radiation dose to animals is not calculated.

As contracted, Renaissance Code Development (RCD) is actively working to comply with Section 508 of the Rehabilitation Act of 1973 (as amended by 29 USC 794d) by conforming to the Act and supporting the requirements of the Standards for Section 508 (36 CFR 1194.1). This conformance is ongoing, and the User will see edits throughout the lifecycle of PiMAL, and other Radiation protection computer code Analysis and Maintenance (RAMP) software, to demonstrate compliance.

The culmination of the PiMAL work, authored by various groups since its inception, is a detailed mathematical phantom model with freely moving arms and legs to enable the analyses of realistic exposure configurations and an accompanying GUI to facilitate phantom postures and dose assessment analyses.

2 INSTALLATION

Installation instructions are provided here for a Microsoft Windows based system. The installation process of PiMAL itself requires downloading and installing the executable file from the NRC RAMP website (https://ramp.nrc-gateway.gov/codes/pimal). Unlike previous versions, the user is not required to have Java installed on their machine; the required Java run-time libraries are included with the installation package.

Once RAMP access has been granted, and the user is logged into the RAMP website, the Download option can be found by navigating to the PiMAL code menu (Figure 2-1).

Step 1. Download the PiMAL executable file.

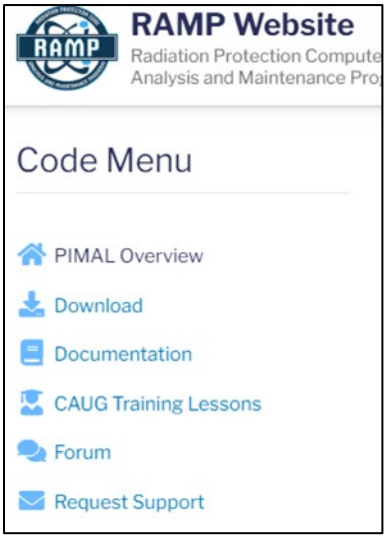

Figure 2-1 Downloading Install Exectuable from RAMP Website.

Step 2. Double-click the zipped .exe folder (Figure 2-2) to download the executable.

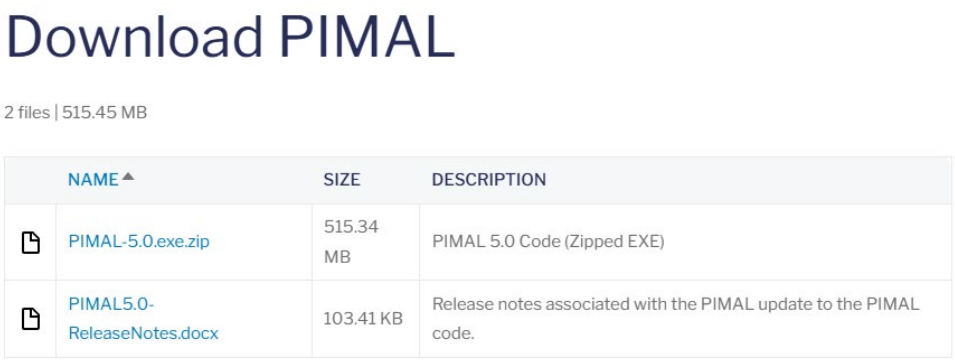

Figure 2-2 Download Options for the PiMAL Executable and its Release Note.

Once downloaded to your computer, open the installer executable to begin the install and setup processes for PiMAL. When installing, a Windows Defender SmartScreen may appear if your computer is so configured. If this occurs, select “More Info” to expand the visible options and hit “Run Away”.

Step 3. Click Next on the Setup Wizard window (Figure 2-3).

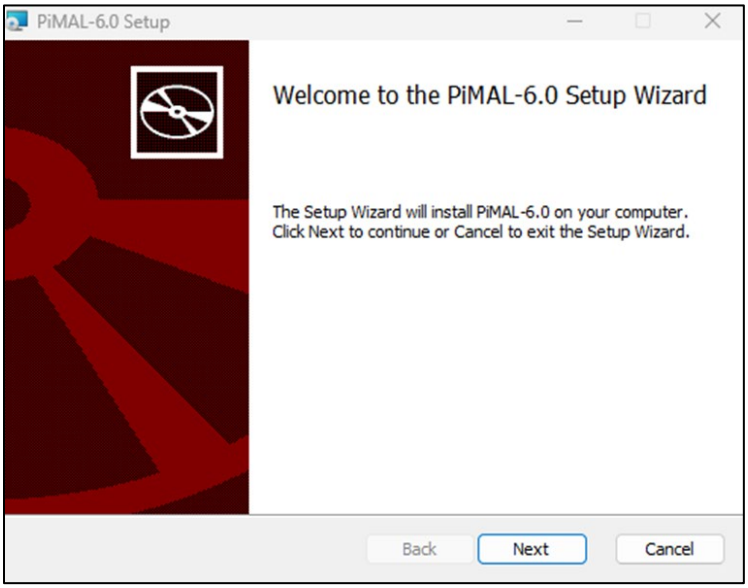

Figure 2-3 PiMAL Setup Main Install Window.

Step 4. Choose your install destination folder (Figure 2-4); this is where the program is to be installed. This is separate from the working directory where program inputs and outputs will be stored. The working directory is defined by the user in a later step.

The default install destination folder for PiMAL is:

C:\Users\<username>\AppData\Local\PiMAL-6.0

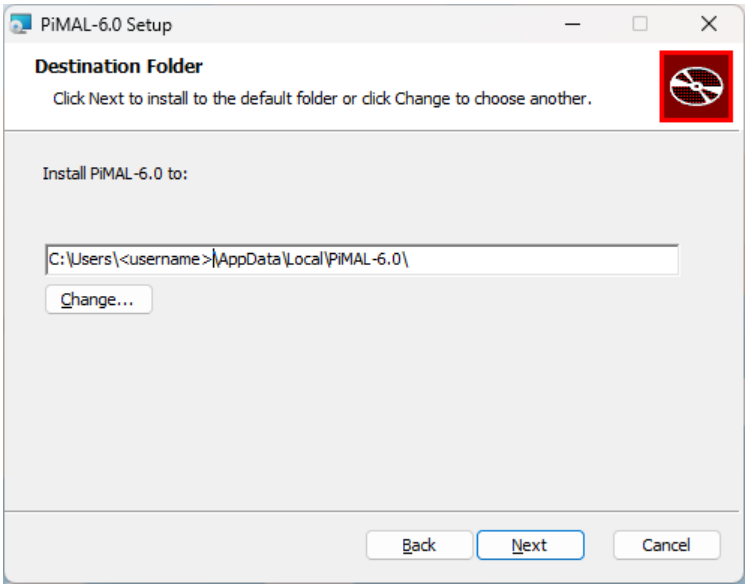

Figure 2-4 Defining PiMAL Installation Directory.

Tip: By default Windows will hide the AppData folder. The user can navigate to this location by explicitly typing the address in Windows explorer address bar or by adjusting the system settings to show hidden files and folders. This can be set by following these instructions: https://support.microsoft.com/en-us/windows/view-hidden-files-and-folders-in-windows-97fbc472-c603-9d90-91d0-1166d1d9f4b5.

Step 5. Click Install (Figure 2-5) to start the installation process.

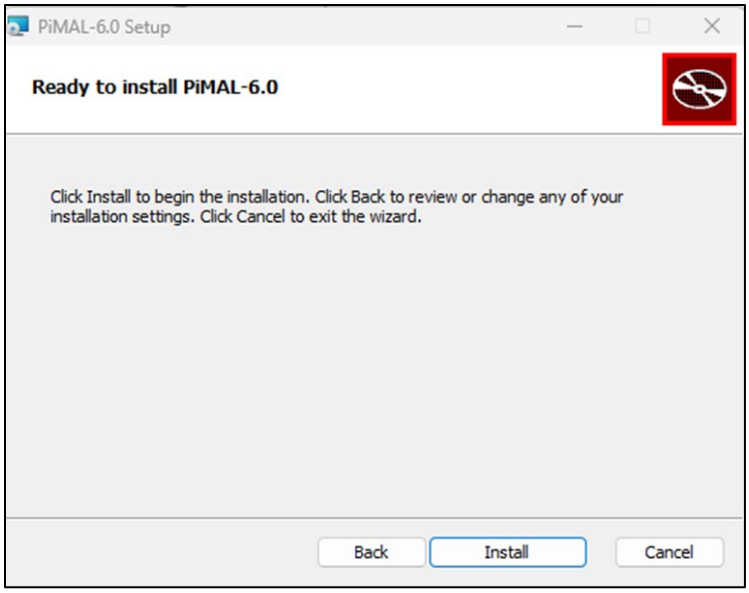

Figure 2-5 PiMAL Setup Install Window.

The window will update to show the progress of the installation. This should take less than a minute.

Step 6. When the setup is complete, click Finish in the Setup Wizard (Figure 2-6).

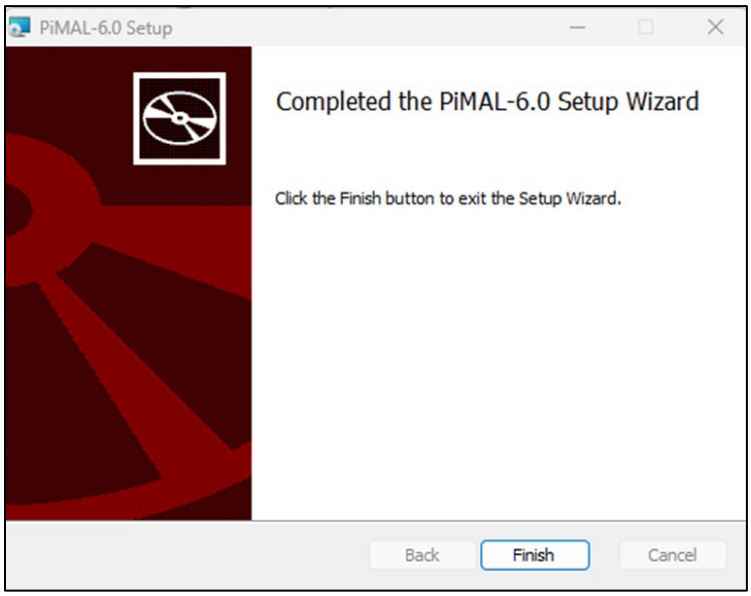

Figure 2-6 PiMAL Setup Window Installation Complete Window.

Step 7. Confirm installation was successful. Once the setup has been completed the following will exist on the user's machine:

PiMAL-6.0 shortcut on the desktop (Figure 2-7)

RAMP Start Menu Folder containing a PiMAL-6.0 shortcut (Figure 2-8)

Figure 2-7 Desktop Shortcut for the Installed PiMAL Executable.

Figure 2-8 RAMP Start Menu Folder Containing a Link to the PiMAL Executable.

Step 8. Double click the PiMAL icon that was created on the desktop or select the link generated in the RAMP Start Menu folder. PiMAL requires 5 to 7 seconds to initialize on opening. Once opened, the simulation input window will be displayed (Figure 2-9).

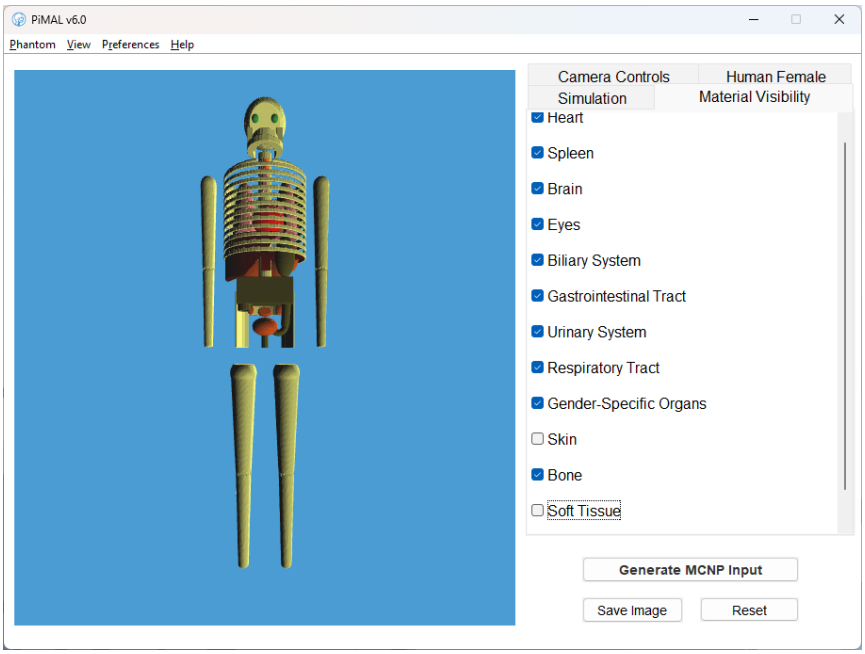

Figure 2-9 PiMAL Simulation Input Window.

3 SOFTWARE CONFIGURATION

Before using PiMAL for the first time, a few customization settings are required to be input by the user. The following sections will walk through:

- setting the working directory where program inputs and outputs are stored;
- setting the path to the MCNP executable; and
- setting the path to the MCNP batch file that sets the environmental variables required for executing MCNP.

Linking PiMAL and MCNP allows the two codes to interface and obtain dose results in a seamless process.

3.1 Setting the Working Directory

As MCNP inputs are created, configurations selected, and MCNP is executed through PiMAL, these generated files need to be saved locally. The user must decide where these files are to be saved by setting the working directory. This directory should be accessible in that administrative level privileges are not required where the user had read and write permissions.

To set the working directory, navigate to the PiMAL toolbar and select Preferences > Change Working Directory.

By default, the current directory will be set to:

C:\Users\<username>\Documents

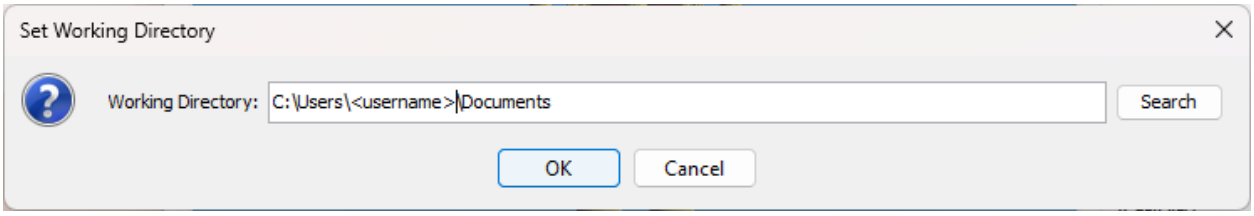

Figure 3-1 Changing Working Directory Window.

Click Select. In the pop-up that follows, navigate to the folder where the files are to be saved.

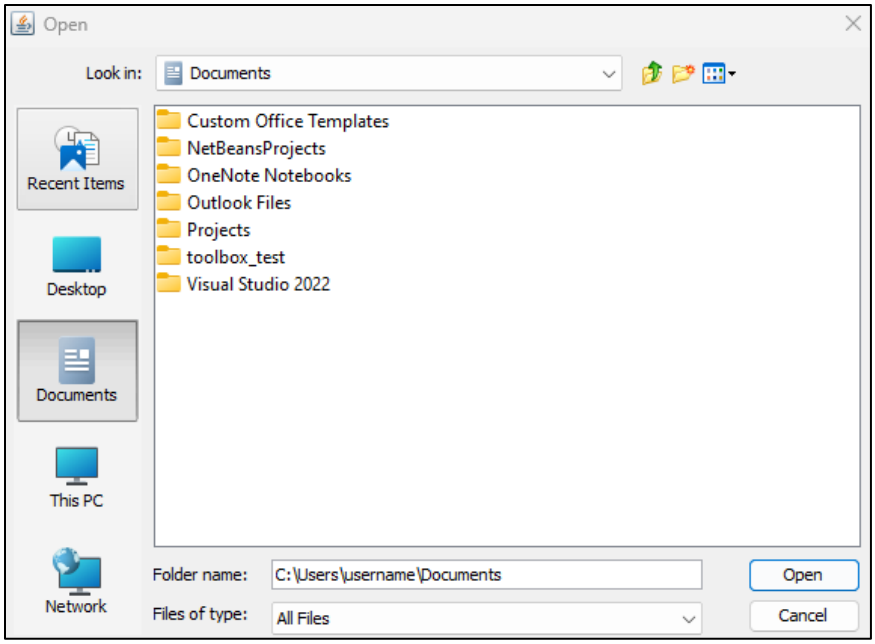

Figure 3-2 Specifying Working Directory Location.

Click on the designated destination folder and press Open.

Click OK on the directory window (Figure 3-1). The working directory folder is now set as the default save folder for PiMAL configurations and MCNP run files.

3.2 Setting the Path for the MCNP Executable

It is assumed the user has successfully installed MCNP on their machine; instructions for that install are not provided here. If MCNP has not yet been installed, please request the code through appropriate channels via the Radiation Safety Information Computational Center (https://rsicc.ornl.gov). MCNP is not required for running the PiMAL GUI (e.g., articulating limbs/positions), but radiation transport is not possible without an installed version of MCNP.

The path to the MCNP executable directory must be set in PiMAL so that MCNP can be called from within PiMAL.

On the PiMAL toolbar, select Preferences > Set MCNP Command.

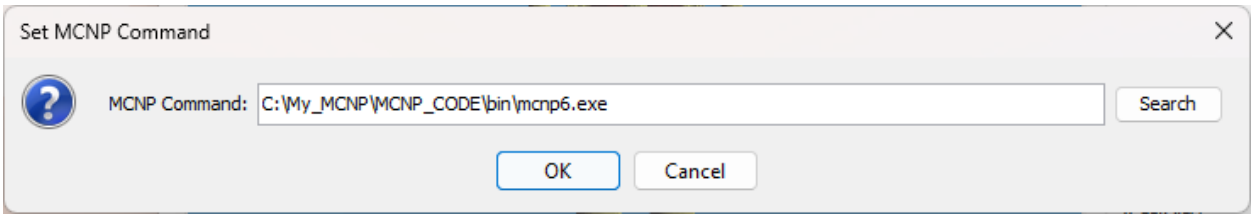

Figure 3-3 Setting the MCNP Executable Location.

The MCNP command must include the absolute path to the executable. If the installation was performed as directed in the MCNP manual, the typical default install location is:

C:\My_MCNP\MCNP_CODE\bin\mcnp6.exe.

If an environmental variable has been set (e.g., mcnp6) it may also be entered here.

If the MCNP location needs to be updated, enter the new install location in the text field and select OK.

> *Tip: To obtain the MCNP installation location, open the MCNP command line shortcut on the desktop and enter: "where mcnp6". The absolute path of the MCNP executable (*.exe) will be returned as well as the location of the environmental variable batch file (*.bat). This paths can be copied and pasted into the path location as necessary.*

3.3 Setting the MCNP Environmental Variable Batch File

The MCNP batch file is generated as part of the MCNP install process depending on the version of MCNP and the user's setup. If not needed it may be left blank. This batch file defines the necessary environmental variables required by MCNP during execution. The typical default install location is:

C:\Users\<username>\mcnp_env_620.bat.

On the PiMAL toolbar, select Preferences > Set Environment Variable BAT to specify where the MCNP batch file is located.

> *Tip: To find the location of the MCNP batch file, right click on the MCNP command line icon on the desktop and select properties. The batch file location is identified under the "details" tab.*

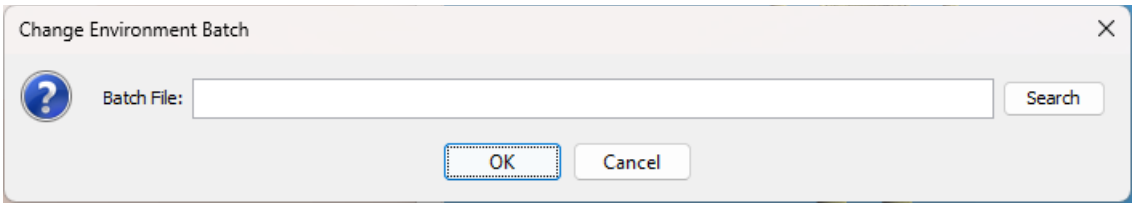

Figure 3-4 Setting the MCNP Environment Variable Batch File Location.

Press Select and navigate to the MCNP batch file. Click on the designated file and press Open.

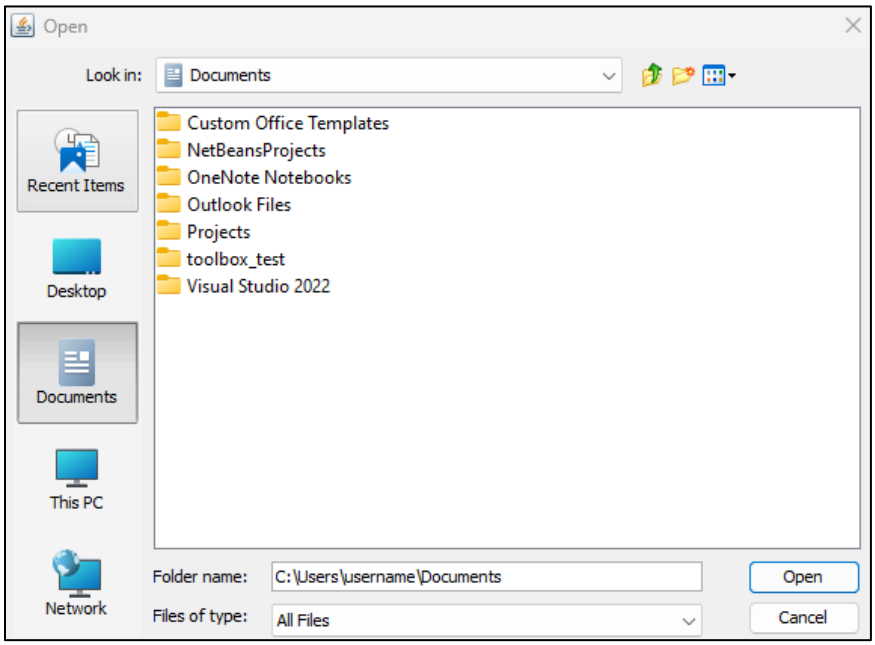

Figure 3-5 Specifying MCNP Environment Variable Batch File Location.

Press OK on the batch window (Figure 3-4) when complete.

MCNP is now configured and can be executed by selecting “Generate MCNP Input” in the lower right corner of the input window. To run a PiMAL-generated input deck through MCNP, select “Run MCNP” (bottom center) on the pop-up window that has opened after selecting Generate MCNP. If MCNP is unable to link to PiMAL, an error message will be displayed in the “MCNP Console” tab; otherwise, the run status of the current problem will be displayed.

4 USER INTERFACE

Once the installation process has been completed and you have configured PiMAL to work with MCNP, PiMAL is ready for use. Of immediate interest is the graphical user interface, or GUI, that allows for the easy customization and display of the phantom. In the following sections, the GUI overview, as well as camera controls and other important elements of PiMAL, will be discussed. Pressing the reset button on the main window will reset the simulation entirely to default (3D) values.

> Warning: Breaking the physical limitations of the phantom has the likely effect of causing fatal errors in MCNP. Please be cautious not to overlap one portion of the phantom with another (e.g., impaling the head with the fist, causing legs or arms to intersect, crossing human features with animal features, etc.).

4.1 GUI Overview

Particular GUI features of interest are noted in Figure 4-1 with numbers 1 through 6. Those numbers point out the following: (1) PiMAL Toolbar; (2) 3D View Tabs; (3) Java3D Environment; (4) Phantom Parameters Tabs; (5) Main Buttons; and (6) Phantom(s) location.

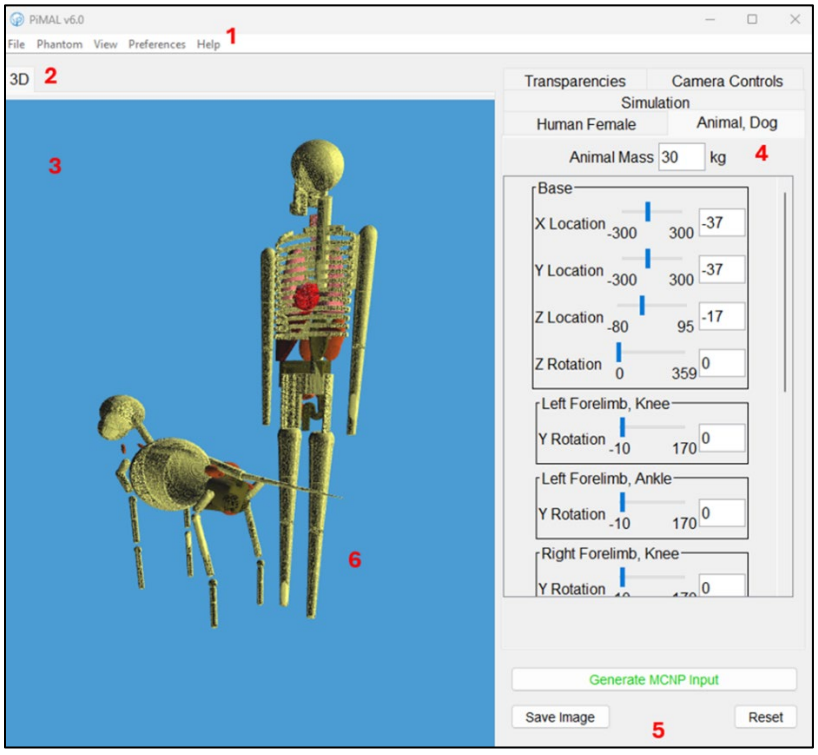

Figure 4-1 Graphical User Interface (GUI).

4.2 3-D Camera Controls

Inside the Java3D environment, the user can change the camera view or its angle using: (1) mouse right-click and drag to rotate camera; (2) mouse left-click and drag to change camera position; and (3) mouse middle scroll to zoom in and out.

In the Camera Controls tab, there is the option to change the zoom rate from 0 to 16, with a default of 8. Lower numbers will zoom with the mouse wheel slower than higher numbers. There is the option to either input the number manually (followed by the enter key), or by using the slider. It is up to the user to decide which method works best for their preferences or situation.

In this tab, there is also the option to change the slew rate. The values you can enter range from -0.5 to 0.5. This will increase or decrease the rate at which the phantom rotates in the Java3D window. The lowest value (+/- 0.01) is the slowest rotation speed and will function to provide the most control over the rotational position of the phantom in the window. Values change the response direction as well as speed; with a negative value, moving the mouse will rotate the image against the direction of the mouse. With a positive value, moving the mouse will rotate the image in the direction of the mouse.

> Note: Changing the rotation, position or zoom of the phantom in the Java3D window does not change the position of the phantom in the MCNP simulation. It is for viewing purposes only, meant to identify how the limbs are positioned, where the companion phantoms are positioned with respect to the human, and any other small details the user wishes to evaluate before starting a simulation.

To reset the phantom's rotation position, click the Camera Reset button in the camera controls pane.

4.3 Human Tab

If the human phantom is selected, the "Human Female" or "Human Male" tab will be shown. If the sliders window is not open on the sidebar, click on the Human (Male/Female) tab to open.

Human tabs include slider and text boxes allowing the movement of the arms and legs for the human. Clicking and dragging the slider for each labeled rotation moves the respective appendage. Experiment with each of the 16 sliders to understand what each one does. It is possible to rotate each of the arms about the shoulder in both the X axis (around the shoulder, parallel to the body) and Y axis (up and down perpendicular to the body) independently. Selecting shoulder rotation moves the whole appendage from the shoulder and selecting the elbow rotation moves just the lower appendage from the elbow. The lower limbs rotate in the same manner.

Using the sliders moves the selected appendage in real time. If you use the text box to enter a value, either hitting “enter”, “tab”, or moving the mouse pointer/cursor out of the text field will update the input value.

It is possible to move the limbs in a way that will impale the limb into the body or the other limbs. Please take care not to do this, as the Java3D window does not account for geometry errors that can occur in the MCNP files. An impaled limb will result in a fatal error when MCNP is run, and no organ doses will be calculated.

4.4 Animal Tab

If an animal is selected from the Phantom drop-down menu, it will appear in the Java3D environment with the human (the human can be removed by de-selecting the human phantom).

PiMAL is not built for the purposes of computing dose to the animals, and as such, when you deselect the human from the JAVA3D environmnent and generate an MCNP input, there are no tallies written to the file. This use case should be for advanced users who wish to manipulate the files with their own knowledge of MCNP.

Figure 4-2 shows the default stance of the phantom, with all sliders at zero position.

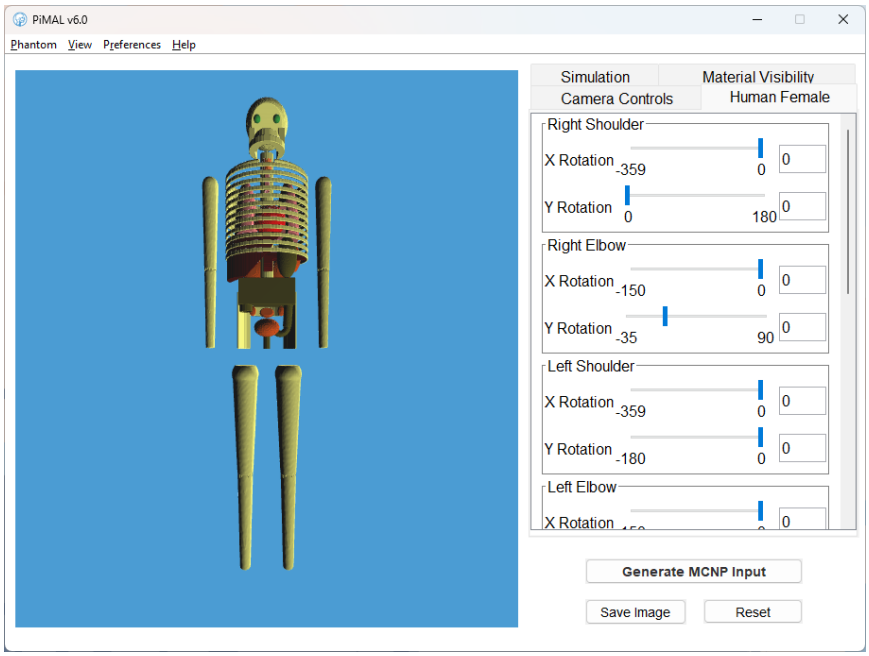

Figure 4-2 Default PiMAL Stance.

There are options to choose from a cat, a dog, or a horse in the phantom selection menu (Figure 4-3). Each has nearly identical bodies, except small changes in face distribution, neck, and leg lengths.

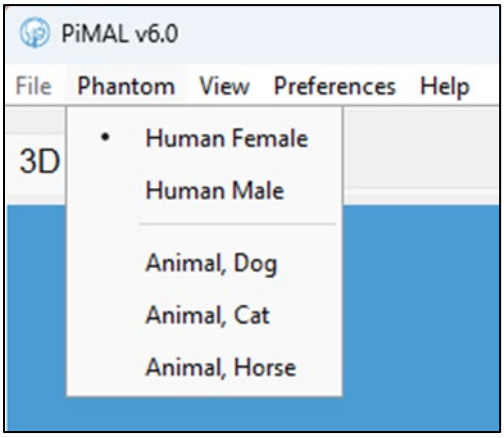

Figure 4-3 Phantom Selection Menu.

Once the animal appears in the Java3D environment (Figure 4-4), the user can select the location and mass of the companion animal by selecting the Animal tab. Much like the human phantoms, the animal phantoms have limb movement capabilities. Inputting limb rotations works similarly to the human phantoms where one can use sliders to angle limbs, or input numbers into the text boxes. Pressing “Enter”, “Tab”, or simply moving the cursor outside of the text box will accept the change in the Java3D environment. Changing the mass of the animal will scale it proportionally and result in an animal with

proportionally sized organs and limbs. The animal type selected will appear in the title of the Animal tab. In the example below, we see we have “Animal, Dog” and its mass is 30 kg.

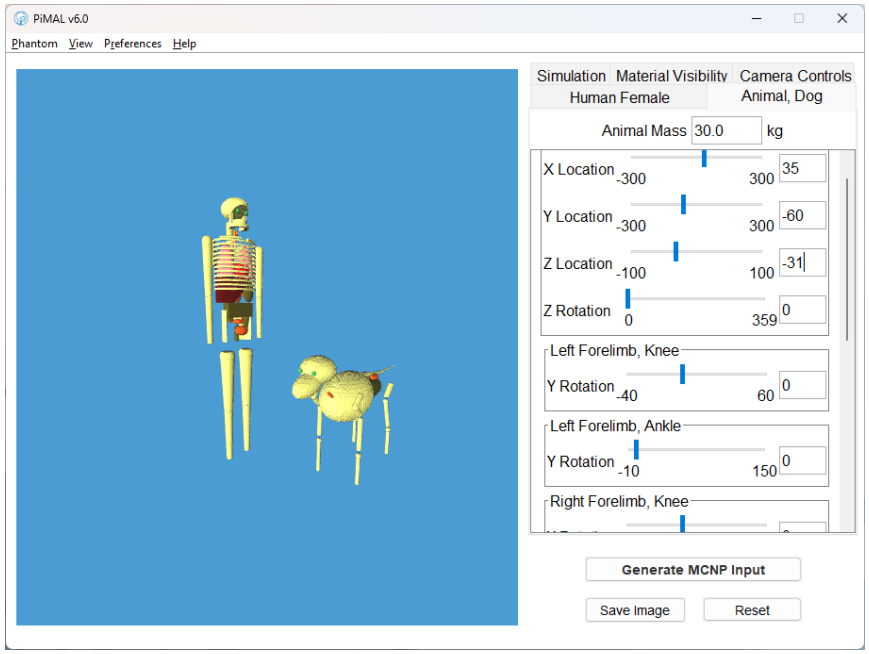

Figure 4-4 Companion Animal Parameter Tab.

4.5 Setting Phantom Visibility

To give access to organ visibilities, select the Material Visibility tab on the sidebar. By checking the box for a given tissue/organ, the tissue/organ becomes visible in the Java3D environment. Unchecking a given box results in the tissue/organ becoming transparent. Unless manually removed by the experienced user, the organ is always present in the MCNP input deck, but simply not visible in the camera image.

Note that the bones have been made transparent in Figure 4-5 (right-hand image).

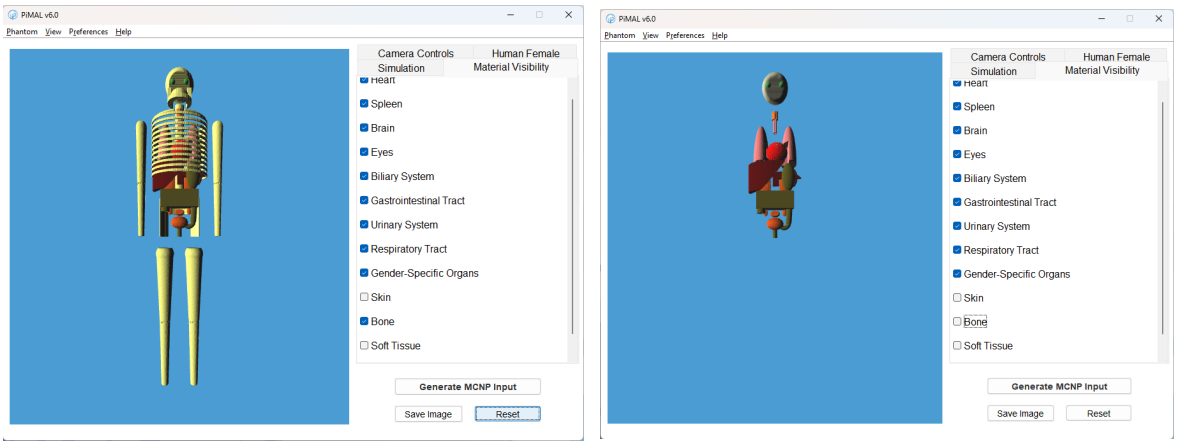

Figure 4-5 Un-checking the "Bone" Visibility Box.

4.6 Resetting the Phantom

Pressing the reset button located in the bottom right corner of the GUI will return the female phantom with all appendage rotations to zero and the transparencies of tissues/organs returned to the default settings. If an animal had been selected, it will be removed from the Java3D environment as part of the reset.

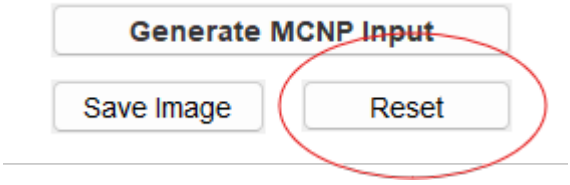

Figure 4-6 Reset Button.

To return the camera view angle to its original position, click on the "Camera Reset" button in the "Camera Controls" tab.

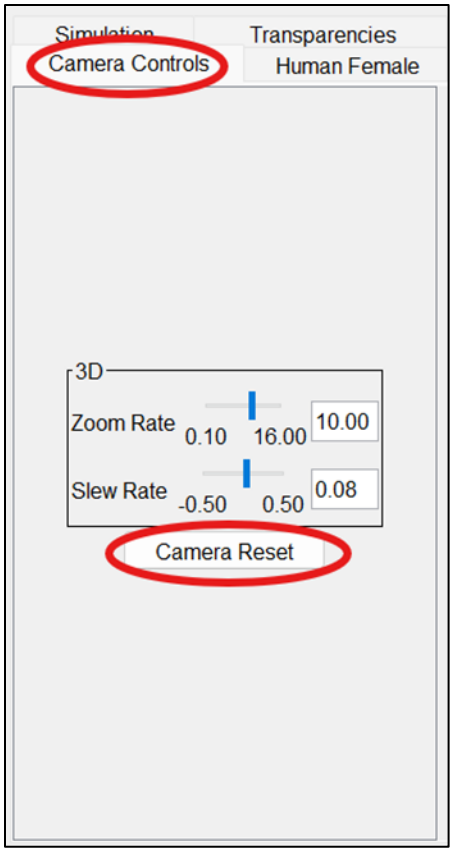

Figure 4-7 Camera Reset Button.

> Note that resetting the camera and the phantom will not change any values the user selected for **Zoom Rate** or **Slew Rate** in the camera controls tab, nor will any simulation parameters in the **Simulation Tab** be reset.

If an animal is selected and the user changes its mass, PiMAL's default behavior is to reset its position relative to the human. If the user prefers the animal's position remain fixed while changing the mass, de-select that option from the preferences menu.

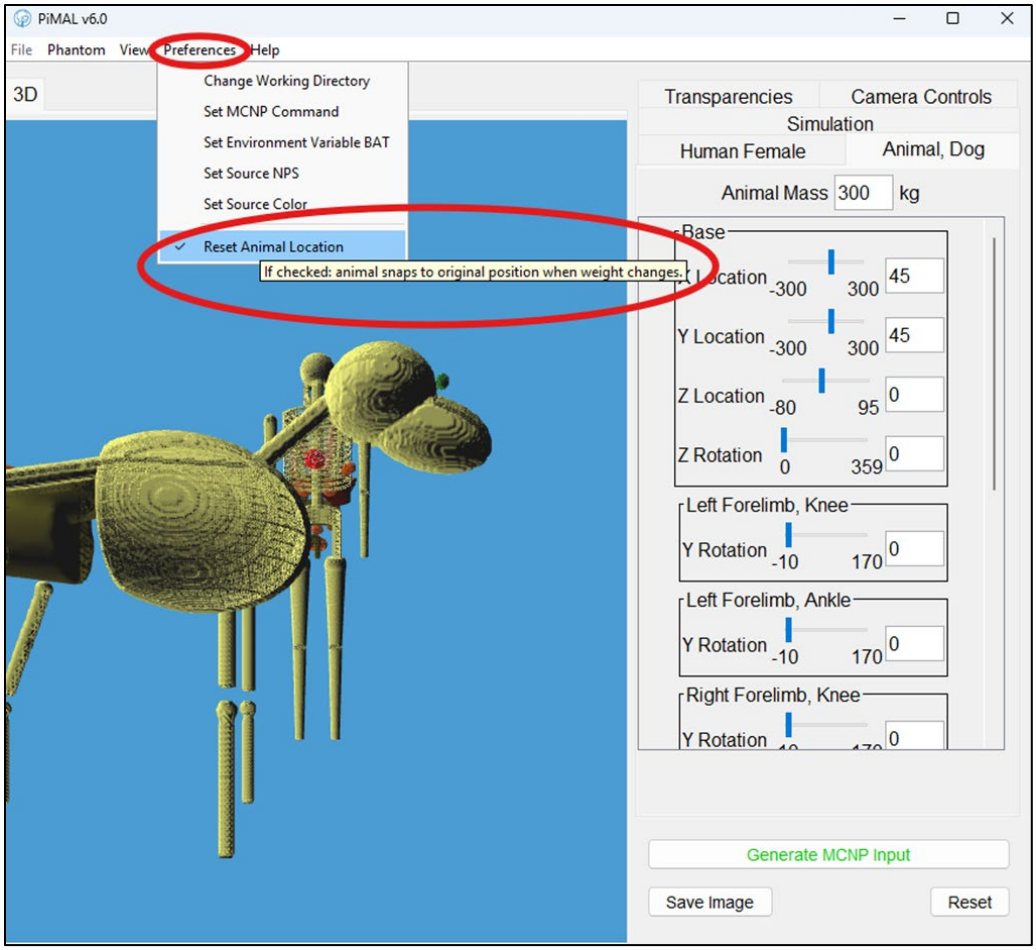

Figure 4-8 Animal Location Reset Button.

5 BUILDING THE MCNP SCENARIO

Once the positioning of the phantom(s) is complete, the next step of the process is to generate the MCNP input deck. This includes defining a source, allowing PiMAL to generate the file, displaying source points for source validation, and saving the input. Custom source creation is introduced in this section. Most of this section will deal with the Simulation tab in the right-hand sidebar (Figure 5-1).

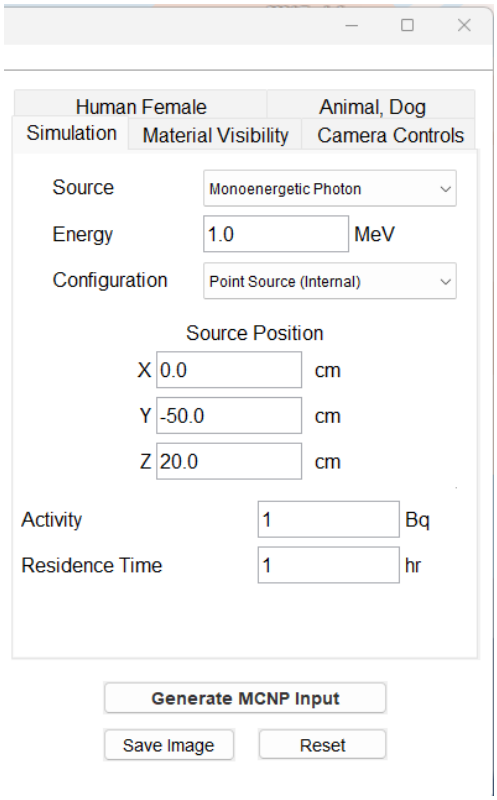

Figure 5-1 Depiction of Simulation Tab on Sidebar.

5.1 PiMAL Built-in Source Settings

PiMAL contains numerous built-in sources for user convenience. These databases will be updated with more source options as time goes on. Currently available source distribution options are: (1) monoenergetic photons or neutrons; (2) radionuclide photon emissions (Co-60, Sn-117m, I-131, Cs-134, Cs-137, Lu-177, and Ir-192); (3) X-ray emission spectra (60, 80, 100, and 120 kVp); and (4) (α,n) reaction neutron sources (AmBe and PuBe). The advanced user can add their own source distributions, as necessary.

The Configuration drop-down menu is for the selection of a source location, or geometry. The configuration options are:

- Point source: the source is location as a point defined by the position entered in the X, Y, Z text boxes;
- Anterior-Posterior (AP): particles enter the phantom through the front (anterior) surface and exit through the back (posterior) surface;
- Posterior-Anterior (PA): particles enter the phantom through the back surface and exit through the front surface;
- Left/Right Lateral (LLAT/RLAT): particles enter the phantom through the left or right lateral surface exiting on the opposite side;
- Isotropic: the source is located on a spherical surface surrounding the phantom; and
- Internal Organs: the source is located in a specified organ. If a companion animal is selected, additional source location options for animal internal organs will be present.

The default number of particle histories is 100,000. The user can change this value in the Simulation tab. If other source inputs are desired, the advanced MCNP user can select one of the above options and then modify the input deck or build their own source data.

The pre-built source definition and configuration combinations allowed are identified in Figure 5-2.

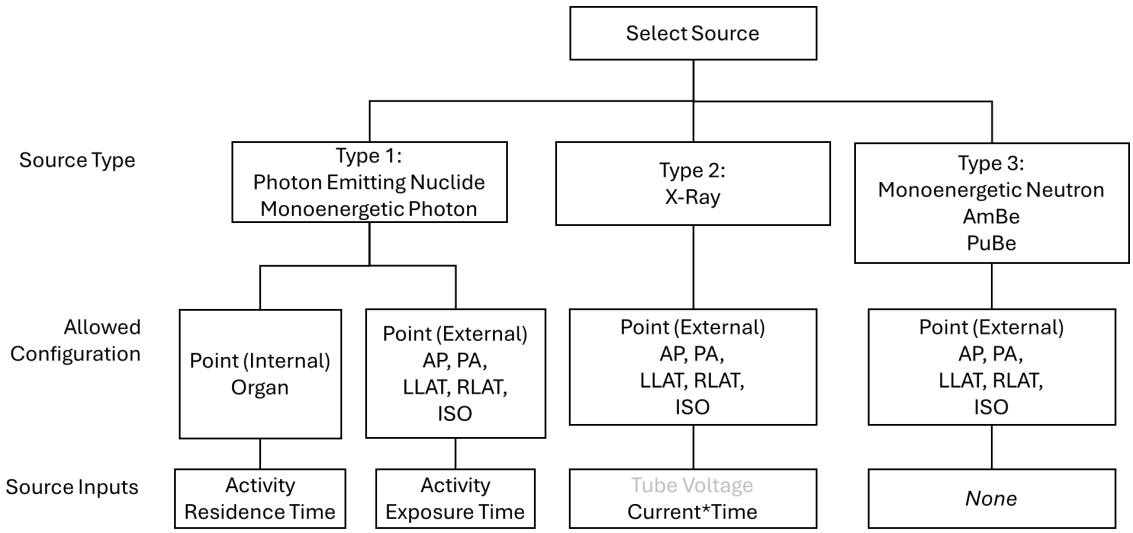

Figure 5-2 Allowed Source Type and Configuration Combinations.

5.2 Generating MCNP Input

To generate the MCNP input deck, press the Generate MCNP Input button (Figure 5-1). Figure 5-3 shows an example of the MCNP input window that results from pressing the Generate MCNP Input button. The contents of the MCNP input deck can be edited

through the input window using the built-in text editor. Changes made to the input deck will be saved and used in the current MCNP run.

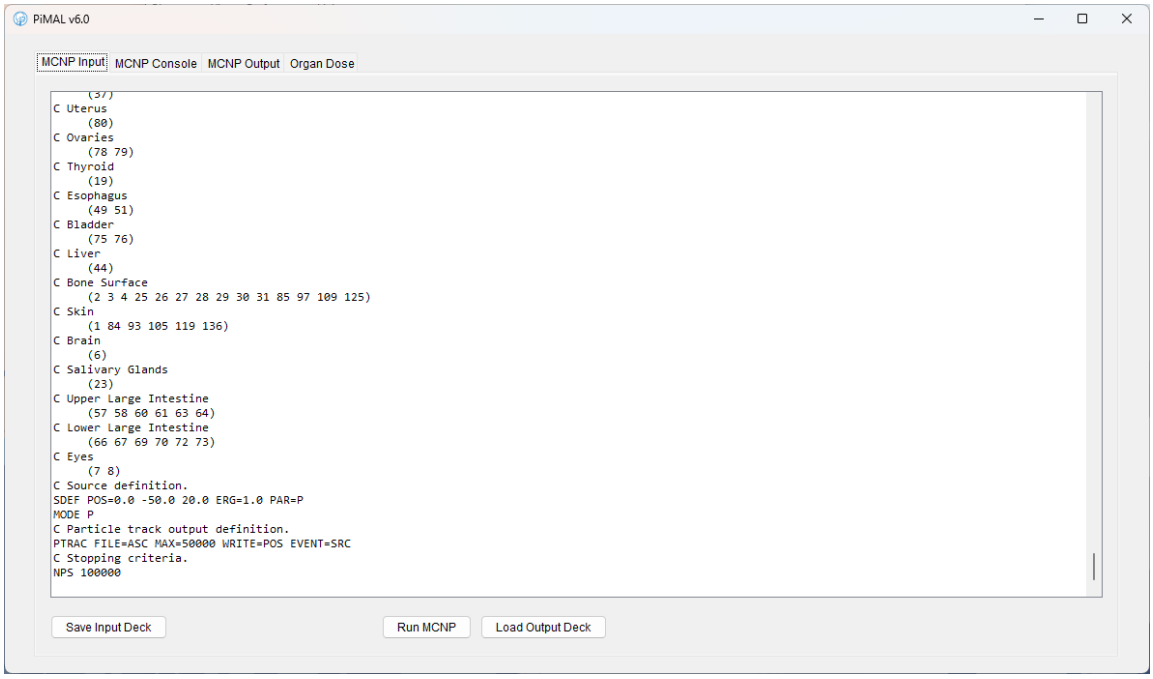

Figure 5-3 MCNP Window.

5.3 Displaying Source Points

Source points will automatically display in the Java3D environment once a successful MCNP simulation is run (Figure 5-4). This is a convenient way to visualize the geometry of the source in and around the phantom. The user can disable the source display feature through the View drop-down menu (Figure 5-5).

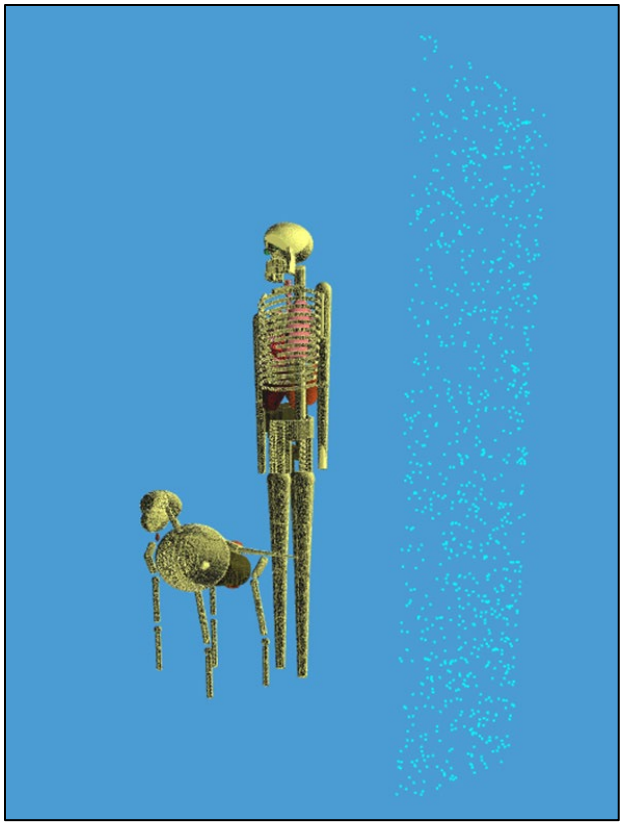

Figure 5-4 Source Point Display of LLAT Geometry with Companion Animal.

Adjustable settings for source display are:

- Source Display Color: The color of the displayed source points can be set and changed in Preferences > Set Source Color; and
- Display Source Particles: The user can toggle on/off display of source locations in View > Display Source Particles. This will automatically show source particles when an MCNP run has finished successfully.

If a given source emission point happens to fall directly on a defined MCNP surface, MCNP will end in a failed run. An unsuccessful simulation will result in a blank dose form (Figure 5-6).

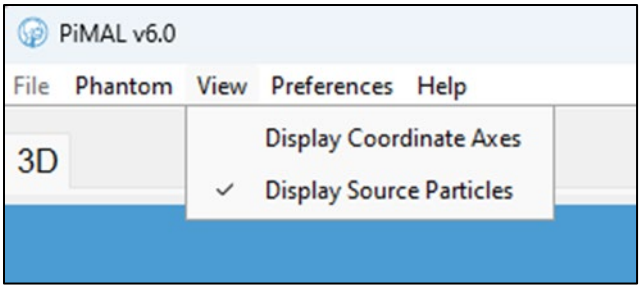

Figure 5-5 Source Particle Display Option.

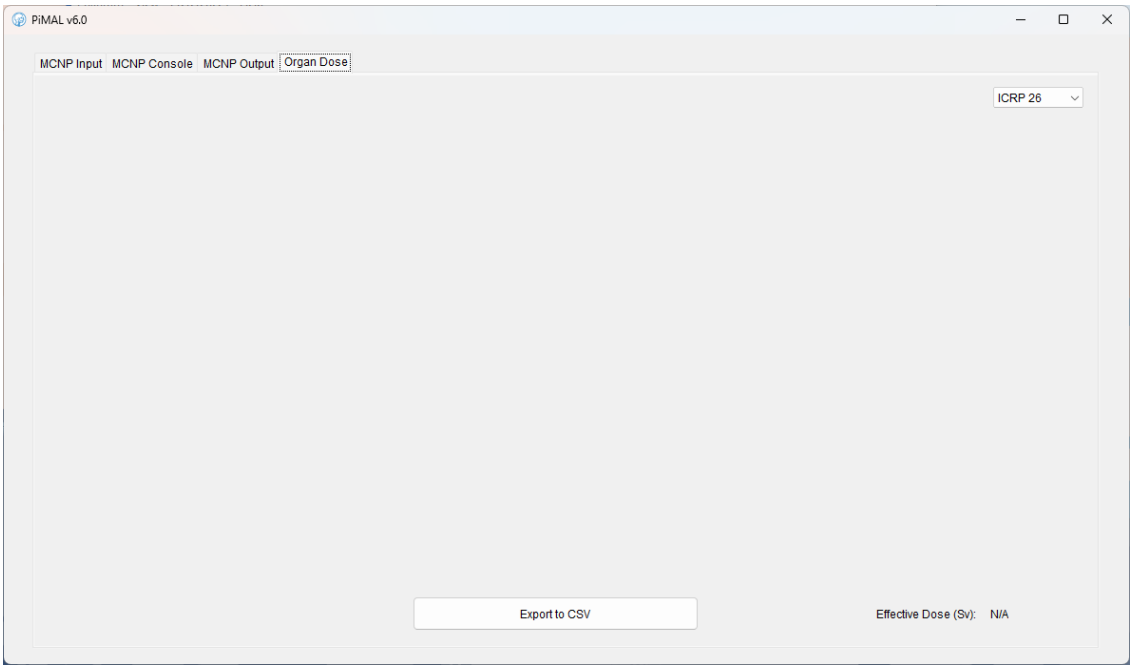

Figure 5-6 Blank Dose Form Indicating an Unsuccessful MCNP Simulation.

5.4 Saving Input

To save the MCNP input deck, navigate to the button at the bottom of the MCNP terminal screen (Figure 5-3). Press Save Input to open the save dialog window (Figure 5-7):

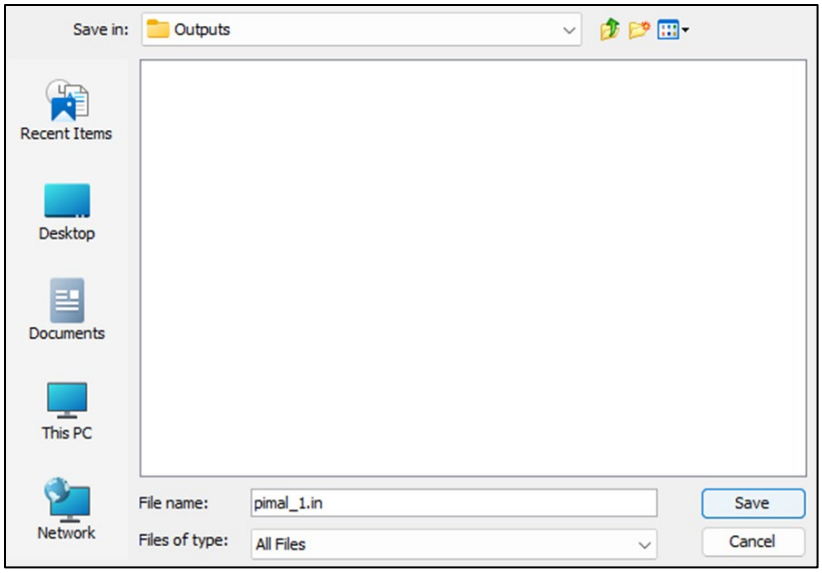

Figure 5-7 Save Input Window.

In this window, enter the file name and press save to complete the process.

5.5 Steps to Entering Custom MCNP Configurations

PiMAL contains a few optional sources for simulation, but other sources may be desired. When the need arises, a source may be defined manually.

The steps for entering a custom source are outlined as follows:

1. save the MCNP input deck and open the new, custom source file in a text editor, or edit within the Generate MCNP Input window using the built-in text editor;
2. make changes to the Materials card (addition of materials);
3. make changes to Cell/Surface cards with inclusion of materials;
4. adjust the source definition (SDEF); and
5. save the new source input deck.

If the tally specifications have not been altered (including syntax), running an edited version of the MCNP input deck should be possible. This will still make available organ tally information in the MCNP terminal screen, as well as source points in the Java3D screen (if selected in the view menu).

MCNP will not run radiation transport and will not result in an answer if a cell, surface, or material has the same number as one already defined in the input deck. For this reason, if you add to a phantom, you must ensure that numbering does not overlap. For example (see Table 5-1), if adding to female phantom geometry, you must use cell numbers greater than 132, surfaces greater than 338, etc.

Table 5-1 Base Index Numbers for Placing Cells, Surfaces, or Materials.

	Cell Numbers	Surface Numbers	Material numbers
Female Phantom	1-132	1-338	1-25
Male Phantom	1-134	1-305	1-25
Animal Phantoms	200-259	2000-2353	1-25

6 RUNNING MCNP

PiMAL creates an MCNP input deck based on settings provided by the user. The next step is to run MCNP using the new input deck and extract dose tallies. In this section, the options for running a PiMAL-generated MCNP input deck and viewing the organ doses from the MCNP output deck are presented.

6.1 Executing the MCNP code through PiMAL

MCNP can be executed through PiMAL without having to use the MCNP command line. Once the user has phantom(s) arranged, click the Generate MCNP Input button (lower right corner of the PiMAL input screen, see Section 5.2) to create the input deck and display it in the MCNP operations panel (Figure 6-1). The operations panel can be treated like a text editor in that the user can make changes to the file directly in the panel. These edits, however, are not saved to the input deck unless the user explicitly clicks the Save Input Deck button in the lower left of the operations panel.

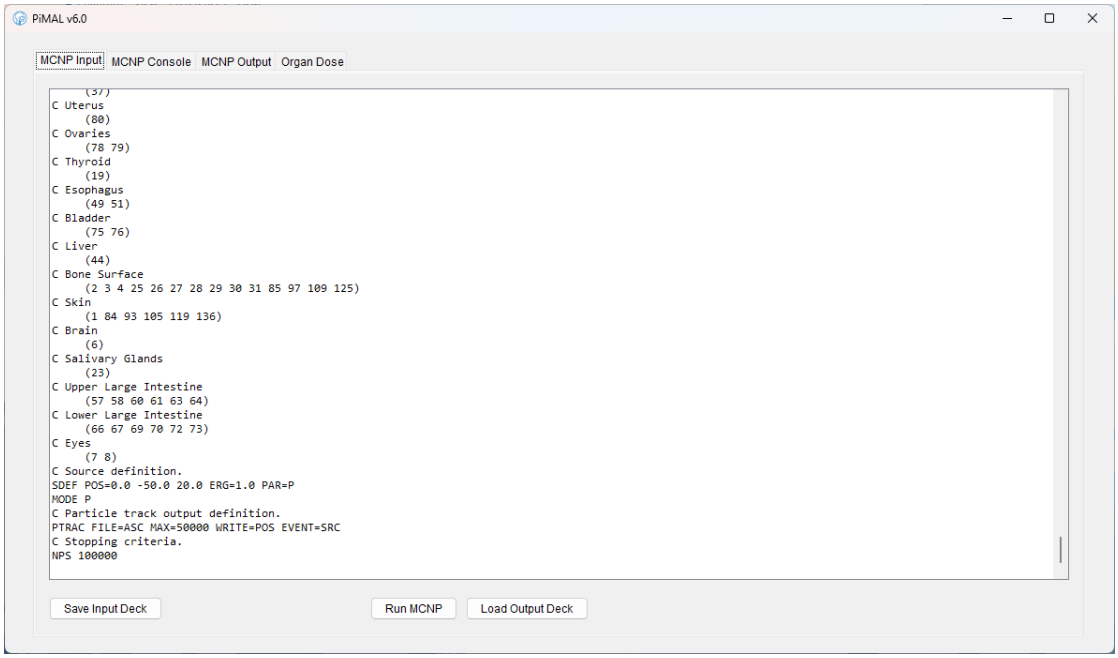

Figure 6-1 MCNP Operations Panel.

The operations panel displays the input deck by default but can also be used to view the MCNP Console, the MCNP Output Deck, and the Organ Dose panel by selecting one of the tabs across the top. The user can also run the MCNP executable and load a previous MCNP output deck for dose analysis using the buttons along the bottom of the panel (Figure 6-1). The uploaded MCNP output deck must be one that PiMAL originally generated; any other MCNP output will result in an error. PiMAL will direct the user to select the appropriate file and will then operate on that file to generate a table of organ doses and effective dose in the same manner as if the output had just been generated

using PiMAL/MCNP. The user is cautioned that when loading a previously run file, a warning will likely appear stating that the corresponding Particle Track Output (PTRAC) file cannot be loaded, however this does not affect the loading of data and subsequent dose calculations provided by PiMAL.

To run MCNP, the user clicks the Run MCNP button at the bottom center of the operations panel. While MCNP runs in the background, the output deck is continuously updated and shown in the MCNP Output Deck tab (Figure 6-2). Until MCNP has fully completed its execution, closing the operations panel will abort the run.

> Note: If a user tries to run MCNP through PiMAL without having an installed version of MCNP on their computer, PiMAL will get stuck in a loop searching for the executable. This loop can be terminated by closing the operations panel.

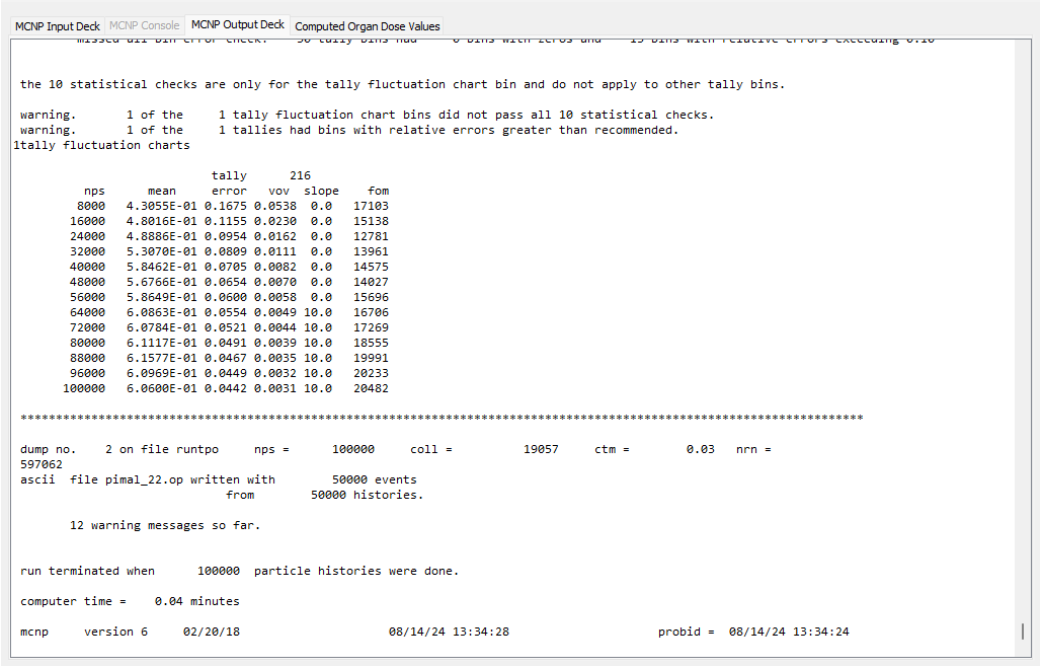

Figure 6-2 MCNP Output Deck.

If errors occur during the MCNP run, a note will be shown in a dialogue box and the MCNP Output Deck will be updated with an error description (Figure 6-3). Select OK to continue. Additionally, MCNP Errors/Warnings are shown in the MCNP output window (Figure 6-4).

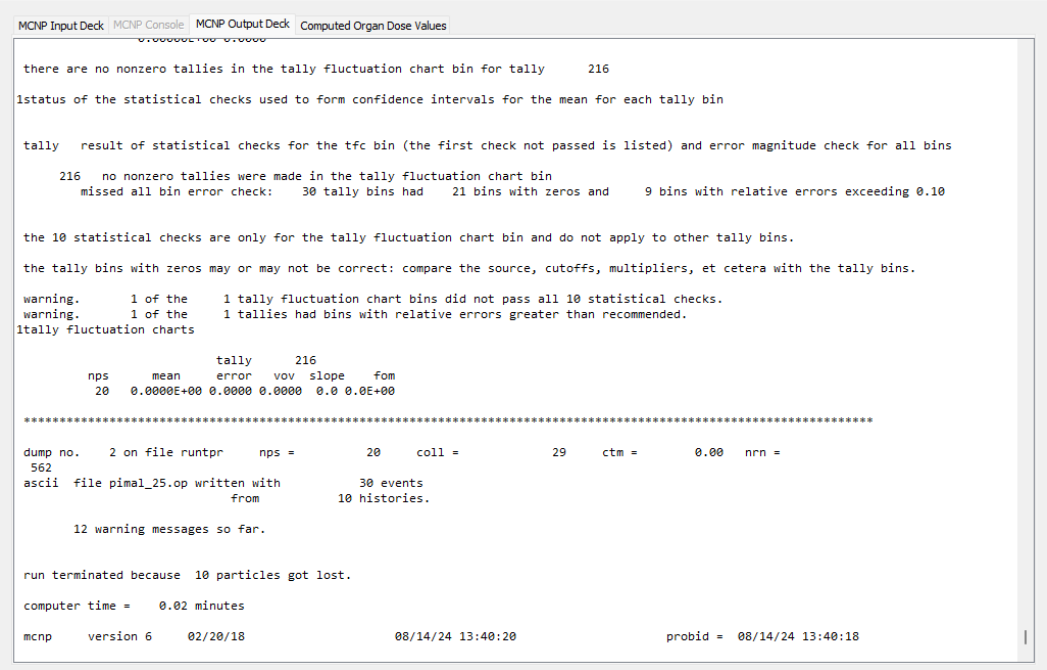

Figure 6-3 An Example of a Lost Particle Termination Warning.

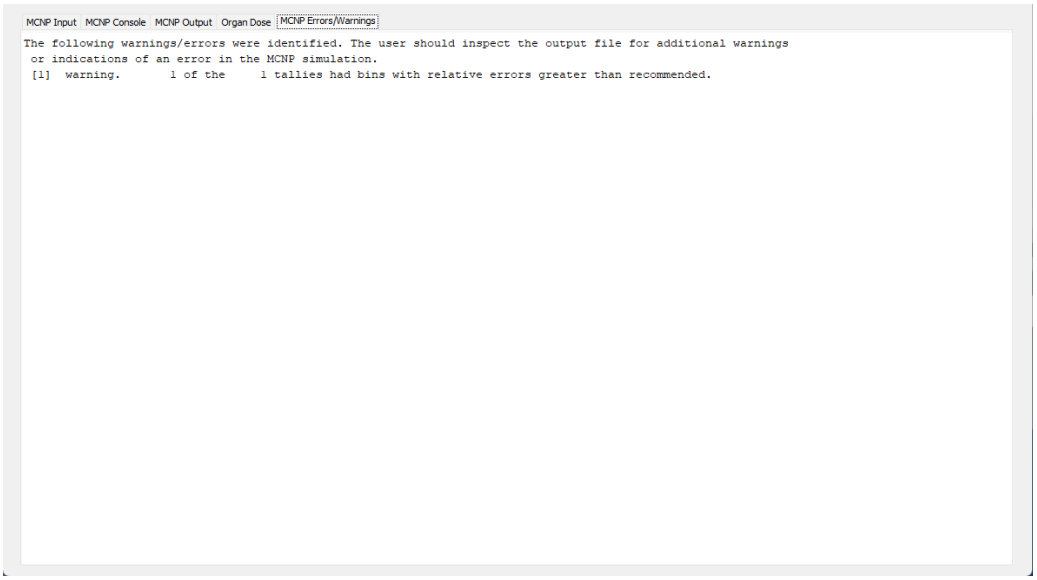

Figure 6-4 MCNP Errors/Warnings Display.

On completion of the MCNP run, a chart displaying Organ Doses (Figure 6-5) is created automatically. This chart summarizes the simulation by providing the organ absorbed dose (with modification thereof described in the next section) delivered to each of 29 organs in the selected PiMAL human phantom along with the relative standard error (as a percentage) of the Monte Carlo calculation of organ dose. Tissue weighting factors are

specified for organs included in the effective dose calculation for the selected ICRP publication (ICRP 1977; ICRP 1991; ICRP 2007).

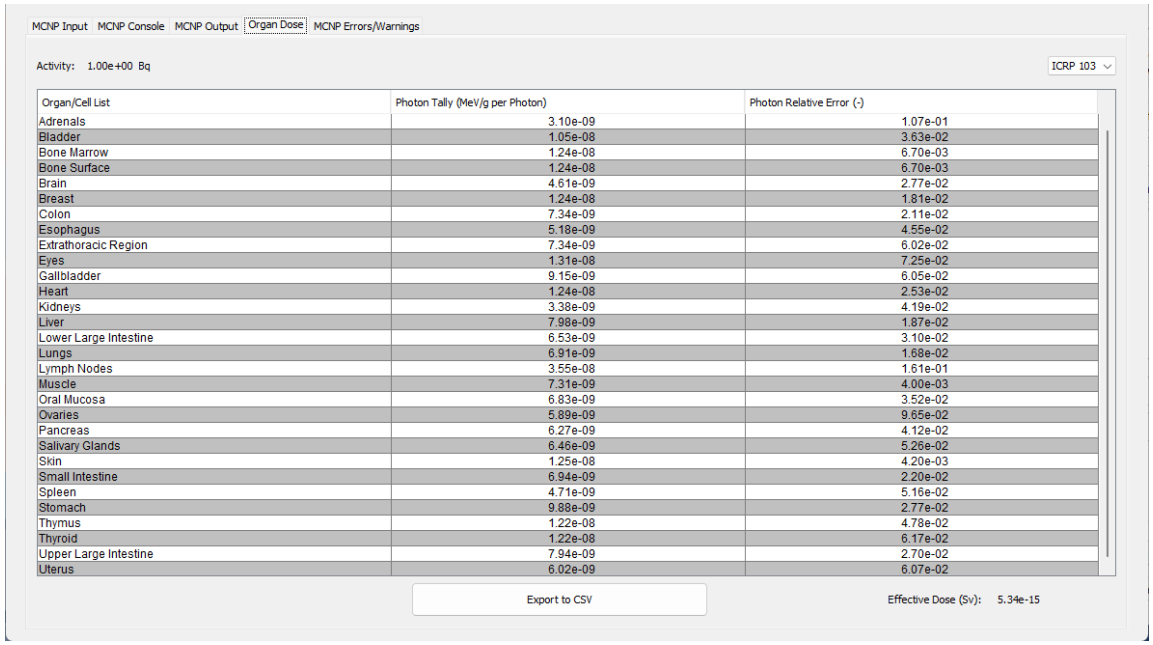

Organ/Cell List	Photon Tally (MeV/g per Photon)	Photon Relative Error (-)
Adrenals	3.10e-09	1.07e-01
Bladder	1.05e-08	3.63e-02
Bone Marrow	1.24e-08	6.70e-03
Bone Surface	1.24e-08	6.70e-03
Brain	4.61e-09	2.77e-02
Breast	1.24e-08	1.81e-02
Colon	7.34e-09	2.11e-02
Esophagus	5.18e-09	4.55e-02
Extrathoracic Region	7.34e-09	6.02e-02
Eyes	1.31e-08	7.25e-02
Gallbladder	9.15e-09	6.05e-02
Heart	1.24e-08	2.53e-02
Kidneys	3.38e-09	4.19e-02
Liver	7.98e-09	1.87e-02
Lower Large Intestine	6.53e-09	3.10e-02
Lungs	6.91e-09	1.68e-02
Lymph Nodes	3.55e-08	1.61e-01
Muscle	7.31e-09	4.00e-03
Oral Mucosa	6.83e-09	3.52e-02
Ovaries	5.89e-09	9.65e-02
Pancreas	6.27e-09	4.12e-02
Salivary Glands	6.46e-09	5.26e-02
Skin	1.25e-08	4.20e-03
Small Intestine	6.94e-09	2.20e-02
Spleen	4.71e-09	5.16e-02
Stomach	9.88e-09	2.77e-02
Thymus	1.22e-08	4.78e-02
Thyroid	1.22e-08	6.17e-02
Upper Large Intestine	7.94e-09	2.70e-02
Uterus	6.02e-09	6.07e-02

Figure 6-5 Organ Doses.

6.2 Calculation of Organ Dose

After running MCNP, in addition to displaying the output deck, PiMAL parses the output (F6 tallies) and creates a listing of the tallied organ absorbed doses. MCNP calculates the mass of the target organ using the cell volume(s) and material density that define the organ. The average energy deposited per unit mass in the named organ is calculated using the MCNP F6 tally.

Absorbed Dose Calculation. Organ dose is calculated differently for each of three source types as chosen by the user: (1) a source radionuclide; (2) an X-ray tube emission spectrum; or (3) a neutron (α,n) reaction source. In the first case, the user selects a specific radionuclide and is then asked to enter the nuclide activity, A_0, and exposure/residence time, τ. Exposure time is meant for external sources, and residence time is a special intake case for an internal calculation with biological clearance of the radionuclide as a source colloid or fragment that neither dissolves in the body nor enters the blood stream. Radionuclide uptake into the blood stream and systemic distribution throughout the body with retention in different body compartments are not considered by PiMAL because internal dosimetric models and coefficients are widely available for that purpose. Residence time should be calculated using only the biological loss rate constant, λ_b, such that:

$$\tau_b[s] = \frac{1}{\lambda_b[s^{-1}]} \quad [6.1]$$

The user is responsible for estimating the biological residence time (not considering radiological loss). Absorbed dose to organ i, D_i, is calculated for radionuclides using:

$$D_i[Gy] = F6\left[{}^{MeV}/_{g\ \gamma}\right] * \tilde{A}[nt] * P\left[{}^{\gamma}/_{nt}\right] * 1.602x10^{-10}\left[{}^{J\ g}/_{MeV\ kg}\right] \quad [6.2]$$

where

$F6$ = the organ F6 tally returned from MCNP (MeV/g per source particle);

$\tilde{A}$ = integrated activity (i.e., total number of nuclear transitions); and

P = probability of photon emission (all energies) per nuclear transition.

Integrated activity is calculated from:

$$\tilde{A}[nt] = \int_o^{\tau} A_0 e^{-\lambda_e t}\, dt = A_0\left(\frac{1 - e^{-\lambda_e \tau}}{\lambda_e}\right) \quad [6.3]$$

with λ_e representing the sum of rate constants for radioactive (λ_r) and biological loss (λ_b). For an internal source, the integration time is assumed to be infinite. For sources external to the body, λ_b is assumed to equal zero, so that the integration time is equal to the exposure time.

For X-ray sources the user will enter X-ray tube exposure factors including tube voltage (kVp), tube current (mA), and tube energized time, t. From these inputs, PiMAL will predict external dose to the receptor organs (D_i) assuming uniform exposure:

$$D_i[Gy] = F6\left[\frac{MeV}{g\ \gamma}\right] * I\left[\frac{mC}{s}\right] * t[s] * \varepsilon\left[{}^{\gamma}/_{e^-}\right] * 1.602x10^{6}\left[\frac{J\ g\ e^-}{MeV\ kg\ mC}\right] \quad [6.4]$$

Tube current, I, multiplied by time (i.e., total flowing charge) is sometimes represented as "mAs", and a tube efficiency, ε, of 1% is assumed for all calculations in PiMAL. More details on X-ray tubes and their operation can be found in Bushong (2008).

As an example, the X-ray tube photon emissions for an operating peak voltage of 100 kVp (Radiopaedia 2024) results in an energy distribution from near zero to 100 keV (Figure 6-6). The continuous portion of the distribution is the result of bremsstrahlung

photon emissions, and the four peaks are due to characteristic X-rays emitted by the representative target material.

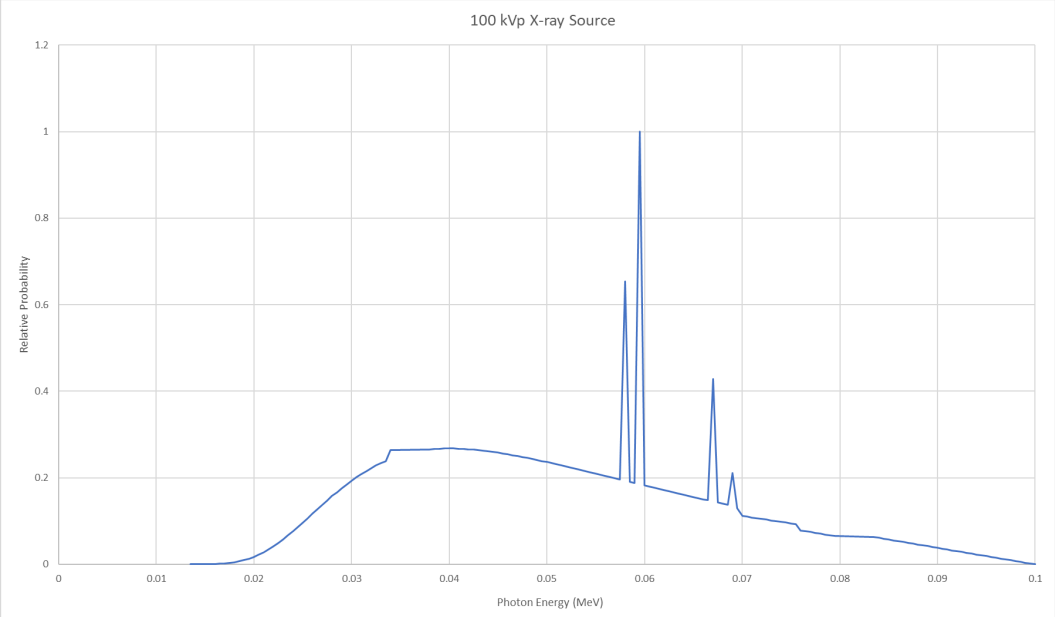

Figure 6-6 X-ray Energy Spectrum from a Tungsten Target Operated at 100 kVp.

For neutron sources no additional scenario data are requested of the user. In this case, the organ dose results (MCNP F6 tally) are presented as dose per emitted neutron [Gy/n] however defined in the scenario.

Calculation of Effective Dose. Once the MCNP run has finished, the organ dose values are displayed on the 4th tab, entitled "Organ Doses" (see Figure 6-5). MCNP generates values for the F6 tally in MeV/g per source particle for the selected exposure scenario, with organ absorbed dose then calculated as described above.

Effective dose (E) is then calculated as the sum of organ-specific absorbed dose (D_i) over all organs i, multiplied by appropriate weighting factors (as specified by the selected ICRP reference), using:

$$E[Sv] = w_r * \sum_i D_i[Gy] * w_{t_i} \qquad [6.5]$$

assuming a radiation weight factor (w_r) of unity (1) for photons and tissue weighting factors (w_{t_i}) from either ICRP 26 (1977), ICRP 60 (1991), or ICRP 103 (2007) (Table 6-1).

Because of the varied definition of radiation weighting factors for neutrons (by energy), and because organ dose by original incident neutron energy is not tracked in MCNP, an

effective dose calculation for neutrons is not possible. It is for this reason that neutron dose by organ remains in units of absorbed dose (e.g., Gy) per source particle. Thus, the present version of PiMAL does not calculate effective doses from neutron sources.

Table 6-1 Tissue Weight Factors for the ICRP 26, 60, and 103 Dosimetry Methods.

Tissue, *i*	**ICRP 26**	**ICRP 60**	**ICRP 103**
Bladder		0.05	0.04
Red bone marrow	0.12	0.12	0.12
Bone surfaces	0.03	0.01	0.01
Brain			0.01
Breast	0.15	0.05	0.12
Colon		0.12	0.12
Esophagus		0.05	0.04
Gonads	0.25	0.20	0.08
Liver		0.05	0.04
Lung	0.12	0.12	0.12
Salivary glands			0.01
Skin		0.01	0.01
Stomach		0.12	0.12
Thyroid	0.03	0.05	0.04
Subtotal	0.70	0.95	0.88
Remainder	0.30	0.05	0.12
Total	1.00	1.00	1.00

In ICRP 26 (1977), the remainder tissue weighting factor has a collective value of 0.30. This remainder weight is applied to the average of the five highest organ doses that are not explicit in the ICRP 26 subtotal column of Table 6-1. The skin and lens of the eye are not included in the remainder tissue calculation. ICRP 60 (1991) states that a weight of 0.05 is given to the average of all remaining organ doses, listing ten organs explicitly to compose the remainder (see Table 6-2). A caveat for the handling of remainder weights in ICRP 60 is that if the highest remainder organ dose is greater than any others, it receives a weight of 0.025 and another 0.025 goes to the average of the remaining organs. And, in ICRP 103 (2007), the remainder weighting factor is increased to 0.12

and should be averaged over the remaining organs as listed in Table 6-2. These rules have been implemented in the PiMAL calculation of effective dose.

Table 6-2 Remainder Organs Listed in the ICRP 60 and 103 Dosimetry Methods.

Tissue	ICRP 60	ICRP 103
Adrenals	X	X
Brain	X	
Extrathoracic		X
Gall bladder		X
Heart		X
Kidneys	X	X
Lymph nodes		X
Muscle	X	X
Oral mucosa		X
Pancreas	X	X
Prostate or Uterus		X
Small intestine	X	X
Spleen	X	X
Thymus	X	X
Upper large intestine	X	

PiMAL gives the user the opportunity to select one of three sets of ICRP tissue weighting factors (ICRP 26, 60, or 103) to calculate effective dose. A dropdown window is provided in the upper right corner of the Organ Dose tab. On selection of a new set of tissue-weighting-factors, the Effective Dose value (lower right corner) will repopulate. The F6 tally chart can be exported as a .csv file by clicking the Export to CSV button at the bottom center of the organ dose window.

7 PHANTOM DESCRIPTIONS

This section contains a description of the cells and the surfaces that make up the components for phantoms modeled in PiMAL. Material definitions and tally descriptions are also provided. The phantoms available in PiMAL include: (1) human female; (2) human male; (3) dog; (4) cat; and (5) horse.

7.1 Human Phantoms

The human phantoms are subdivided into the following component parts of: (1) head and neck; (2) chest; (3) arms; and (4) legs. A pictorial representation of the phantoms is provided in Figure 7-1. The following subsections will provide a detailed description of the human phantoms.

The numbering of cells in the MCNP input deck is maintained between the male and female phantoms. This means that for each of the human phantoms, each organ will have the same number regardless of the phantom's sex. The sex-related organs are similarly numbered but will be in different locations with different parameters and sometimes material. For example, the uterus and the prostate share a cell number between the phantoms but will be defined by surfaces (and have a different volume and material definition) according to the differences between those organs. This is not true of the surfaces used for the organs between the phantoms; surface numbering and parameters will be different between the two sexes.

The following notes apply to both male and female phantoms:

- The material compositions for each component (e.g., heart, lung, etc.) are based on ICRP 89 (2002);
- The density (specific gravity) for each component is based on ICRP 110 (2009);
- The shapes, placement, and subsequently, the volume of each component is determined using basic anatomical knowledge of each organ and has been documented in original literature (Akkurt and Eckerman 2007). The volume of each organ is estimated based on the surfaces used in MCNP, and MCNP computes the mass based on the volume and the density of the simulated organ; and
- Phantoms are based on representative adult male and female values. They do not account for age or weight variation.

Due to the approximation in geometric models of the phantom, it is recognized that resulting calculated volumes may not be exact. The mass of the organ is not necessarily that of the true organ, but rather the mass based on the volume the organ occupies in the mathematical phantom. Since the human phantoms are the targets of interest for determining dose results, it is more important for the density to be correct (ratio of mass to volume) so that organ dose values are correct.

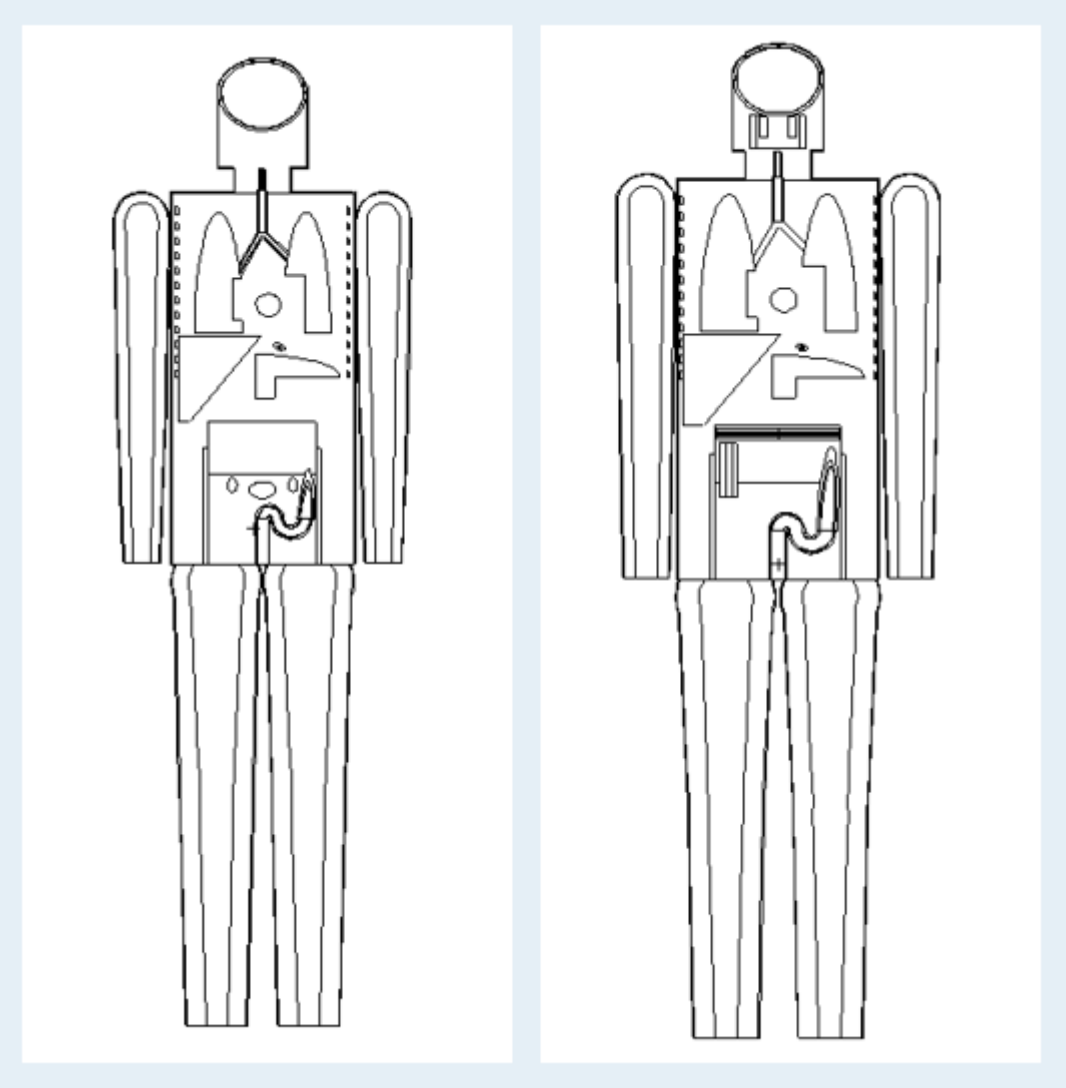

Figure 7-1 Human Female (left) and Human Male (right) Phantom.

This section provides details of the human phantom including: (1) the MCNP cells that make up its components; (2) component material number; (3) component volume; (4) assumed density; and (5) resulting component mass. The male and female phantoms are very similar except for sex-specific organs, relative organ size, and total mass. This section focuses on the female phantom with much of the narrative applying to both phantoms. Specifics that do not appear here can be found in the generated MCNP input deck.

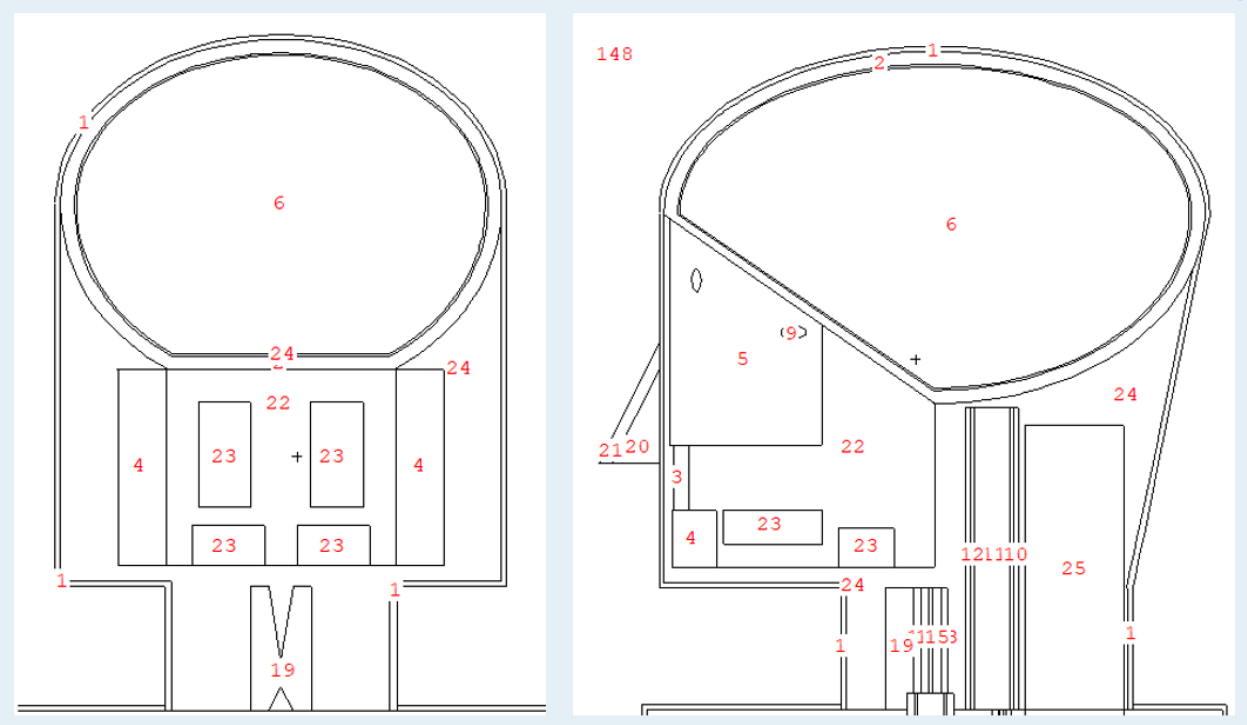

Figure 7-2 2D Female Phantom Head and Neck Diagram (cell numbers shown).

Table 7-1 Female Phantom Head and Neck Component Definitions.

Cell	Component	Material	Volume (cm^3)	Density (g/cm^3)	Mass (g)
1	Skin of Head/Neck	11	214.8	1.09	234
5	Nasal Cavity	5	213.1	1.22	260
6	Brain	6	1310.2	1.04	1360
7	Left Eye	7	6.2	1.07	6.63
8	Right Eye	7	6.2	1.07	6.63
9	Total Sinuses	4	33.1	0.001205	0.0399
10	Pharynx Residual Wall	13	9.71	1.05	10.2
11	Pharynx Contents	4	23.2	0.001205	0.0280
12	Pharynx Mucosa Wall	13	5.41	1.05	5.68
13	Larynx Residual Wall	8	2.53	1.1	2.78
14	Larynx Content	4	3.97	0.001205	0.00478
15	Larynx Mucosa Wall	8	1.35	1.1	1.49
16	Trachea Residual Wall	9	8.67	1.03	8.93
17	Trachea Contents	4	12.8	0.001205	0.0154
18	Trachea Mucosa Wall	12	1.9	1.03	1.96
19	Thyroid	10	11.9	1.05	12.5
20	Nose Contents	4	4.8	0.001205	.00578
21	Nose Wall	13	6.9	1.05	7.25
22	Oral Cavity	12	231.6	1.03	239
23	Salivary glands	12	65.4	1.03	67.4
24	Muscle of Head and Neck	13	1119.9	1.05	1180

The next set of organs described will be those of the axial skeleton (Figure 7-3).

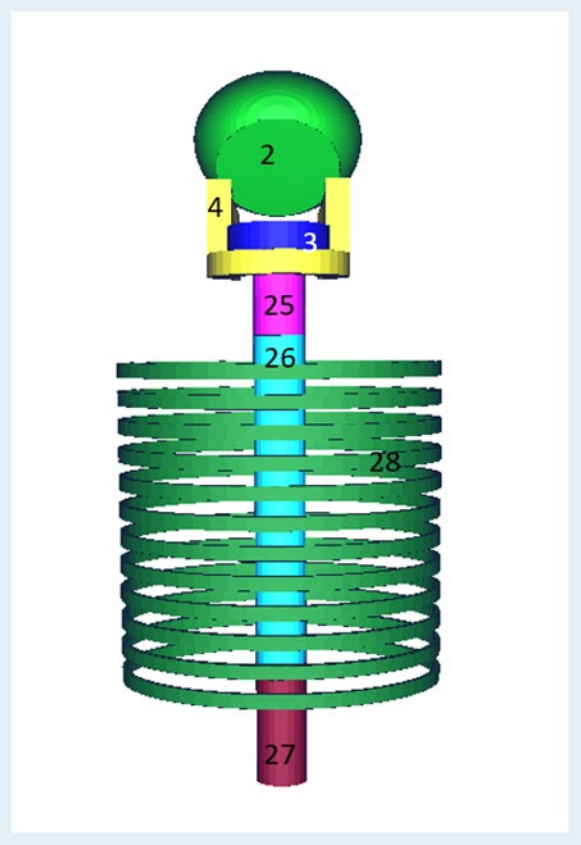

Figure 7-3 3D Axial Skeleton.

Table 7-2 Female Phantom Axial Skeleton Component Definitions.

Cell	Component	Material	Volume (cm^3)	Density (g/cm^3)	Phantom Mass (g)
2	Cranium	2	284.5	1.40	398
3	Teeth	2	30.2	1.40	42.3
4	Mandible	2	144.8	1.40	203
25	Cervical Vertebrae	2	130.6	1.40	183
26	Thoracic Vertebrae	2	418.9	1.40	586
27	Lumbar Vertebrae	2	157.26	1.40	220
28	Ribs	2	531	1.40	743

Following the axial skeleton is the following descriptions of the appendicular skeleton.

Table 7-3 Female Phantom Appendicular Skeleton Component Definitions.

Cell	Component	Material	Volume (cm^3)	Density (g/cm^3)	Phantom Mass (g)
29	Clavicles	2	41.6	1.40	58.2
30	Scapulae	2	154	1.40	216
31	Pelvis	2	460	1.40	644
85	R Arm	2	434	1.40	608
97	L Arm	2	434	1.40	608
109	R Leg	2	1213	1.40	1700
125	L Leg	2	1213	1.40	1700

All cells in Table 7-2 and Table 7-3 are included in the estimation of dose to the bone surface, whereas only cells 25 through 31 are included in the estimation of dose to the red bone marrow.

The chest organs (Figure 7-4) are arranged in the female phantom as follows.

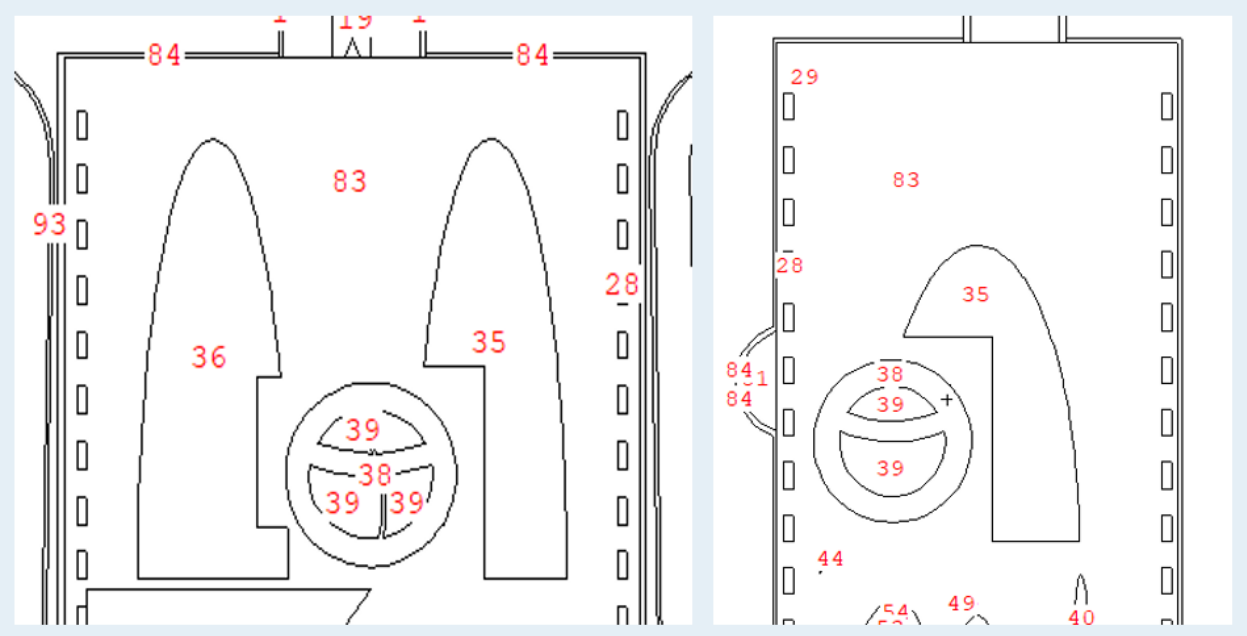

Figure 7-4 Chest Organs of the Female Phantom.

Table 7-4 Female Phantom Chest Organ Component Definitions.

Cell	Component	Material	Volume (cm^3)	Density (g/cm^3)	Phantom Mass (g)
32	Main Bronchi Residual Wall	12	9.827	1.03	10.1
33	Main Bronchi Mucosal Wall	12	10.8	1.03	11.1
34	Main Bronchi Contents	4	2.403	0.001205	0.00290
35	Left Lung	14	1020	0.26	265
36	Right Lung	14	1180	0.26	307
37	Thymus	12	32.725	1.03	33.7
38	Heart Wall	15	231	1.05	243
39	Heart Contents	1	334	1.04	347

The following images and tables describe the abdominal organs (Figure 7-5).

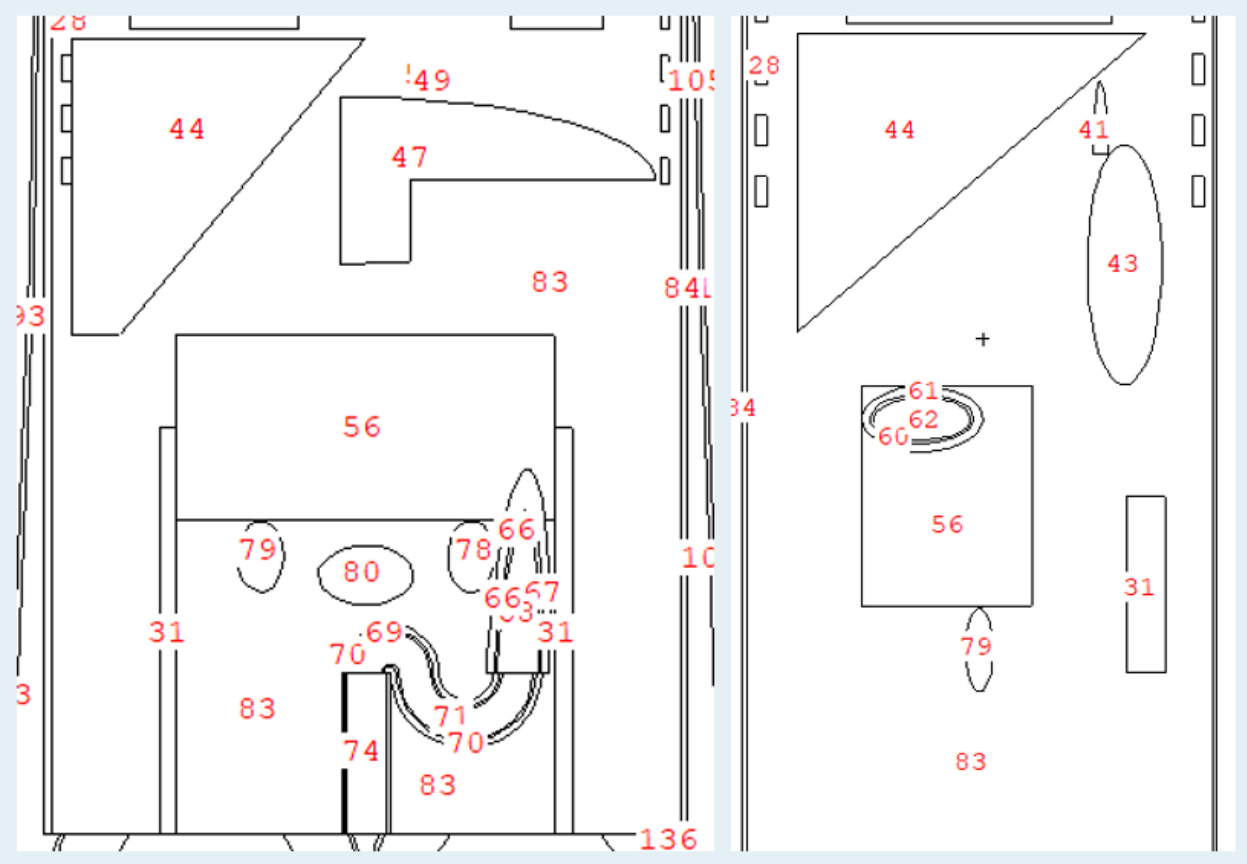

Figure 7-5 Abdominal Organs of the Female Phantom.

Table 7-5 Female Phantom Abdominal Organ Component Definitions.

Cell	Component	Material	Volume (cm^3)	Density (g/cm^3)	Phantom Mass (g)
40	Left Adrenal	12	5.05	1.03	5.20
41	Right Adrenal	12	5.05	1.03	5.20
42	Left Kidney	16	119.2	1.04	124
43	Right Kidney	16	119.2	1.04	124
44	Liver	17	1350	1.05	1420
45	Gall Bladder Wall	12	7.616	1.03	7.84
46	Gall Bladder Contents	12	47.1	1.03	48.5
47	Pancreas	18	98.93	1.04	103
48	Spleen	19	119	1.06	126
75	Urinary Bladder Mucosal Wall	21	5.33	1.04	5.54
76	Urinary Bladder Remainder Wall	21	29.16	1.04	30.3
77	Urinary Bladder Contents	3	154	1.0	154
83	Trunk Muscle	12	24297	1.03	25000
84	Trunk Skin	11	958	1.09	1040

The components of the female gastrointestinal phantom are provided in Table 7-6.

Table 7-6 Female Phantom Gastrointestinal Component Definitions.

Cell	Component	Material	Volume (cm^3)	Density (g/cm^3)	Phantom Mass (g)
49	Esophagus Mucosal Wall	12	5.25	1.03	5.41
51	Esophagus Remainder Wall	12	26.48	1.03	27.3
52	Esophagus Contents	3	7.07	1.00	7.07
53	Stomach Mucosal Wall	20	39.38	1.03	40.6
54	Stomach Remainder Wall	20	73.6	1.03	75.8
55	Stomach Contents	3	187	1.0	187
56	Small Intestine	20	806	1.03	830
57	Ascending Colon Mucosal Wall	20	16.9	1.03	17.4
58	Ascending Colon Remainder Wall	20	52.59	1.03	54.2
59	Ascending Colon Contents	3	73.4	1.0	73.4
60	Proximal Transverse Colon Mucosal Wall	20	11.33	1.03	11.7
61	Proximal Transverse Colon Remainder Wall	20	34.8	1.03	35.8
62	Proximal Transverse Colon Contents	3	48	1.0	48
63	Distal Transverse Colon Mucosal Wall	20	11.3	1.03	11.6
64	Distal Transverse Colon Remainder Wall	20	34.8	1.03	35.8
65	Distal Transverse Colon Contents	3	48	1.0	48
66	Descending Colon Mucosal Wall	20	16.7	1.03	17.2
67	Descending Colon Remainder Wall	20	49.8	1.03	51.3
68	Descending Colon Contents	3	58.93	1.0	58.9
69	Sigmoid Colon Mucosal Wall	20	9.10	1.03	9.37

Table 7-7 Female Phantom Gastrointestinal Component Definitions (Cont.)

Cell	Component	Material	Volume (cm^3)	Density (g/cm^3)	Phantom Mass (g)
70	Sigmoid Colon Remainder Wall	20	28.3	1.03	29.1
71	Sigmoid Colon Contents	3	37.5	1.0	37.5
72	Rectum Mucosal Wall	20	3.85	1.03	3.97
73	Rectum Remainder Wall	20	10.93	1.03	11.3
74	Rectum Contents	3	36.51	1.0	36.51

Female sex organs, which include the ovaries and uterus, are shown below (Figure 7-6).

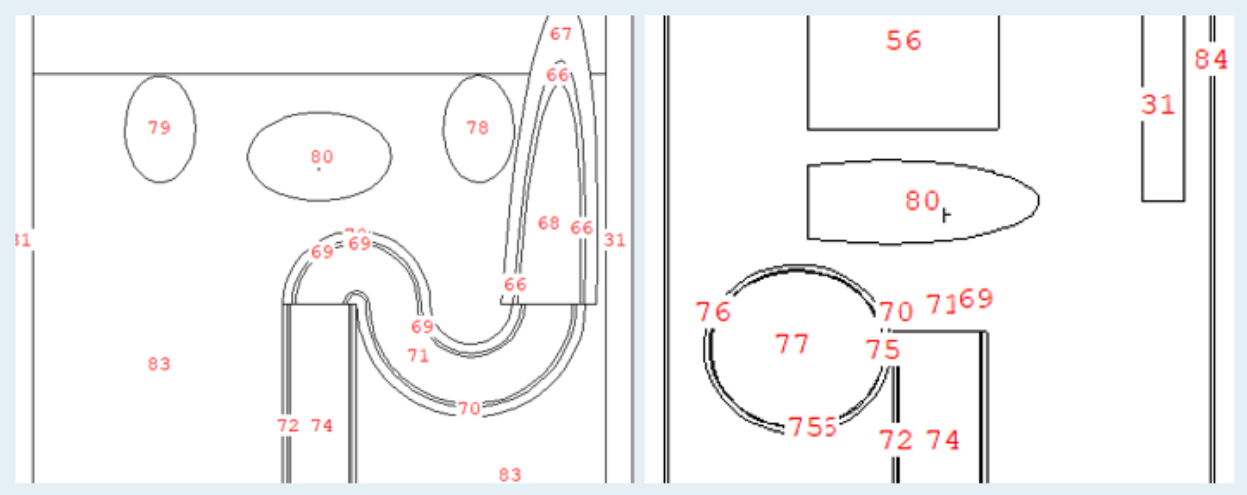

Figure 7-6 Female Sex Organs.

And male sex organs, which include the testes and prostate, are shown in Figure 7-7.

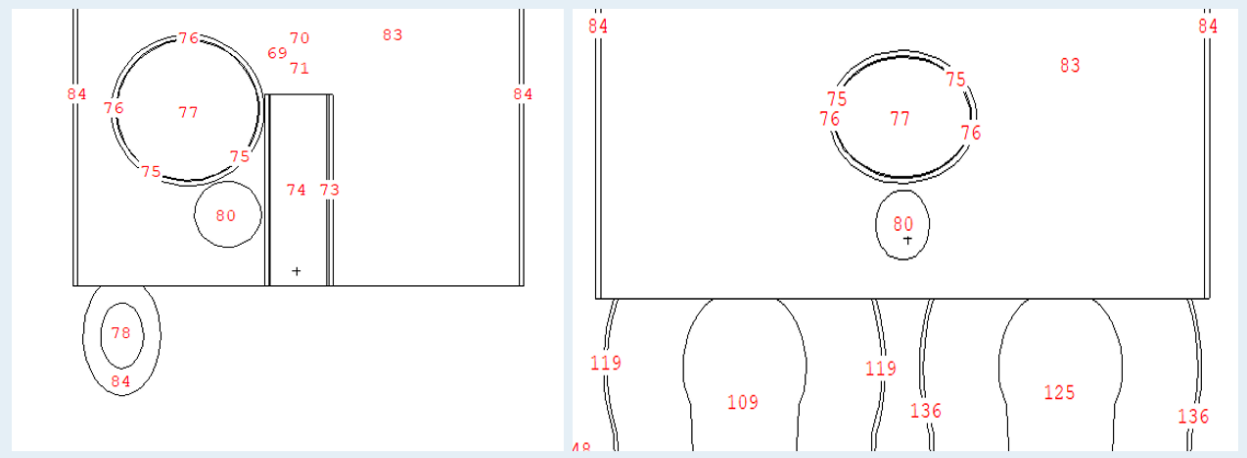

Figure 7-7 Male Sex Organs.

Sex-specific organs include the reproductive organs, as figured above, and the breasts. While both males and females have breast organs, the size of the organ differs from male to female. The volumes and masses of those organs are differentiated in Table 7-8.

Table 7-8 Sex-Specific Organ Component Definitions.

Cell	Component	Material	Female Volume (cm^3)	Male Volume (cm^3)	Density (g/cm^3)	Mass (g)
78	Left Ovary	23	5.05		1.05	5.30
79	Right Ovary	23	5.05		1.05	5.30
78	Left Testes	22		18.8	1.04	19.6
79	Right Testes	22		18.8	1.04	19.6
80	Uterus	24	76		1.02	77.5
80	Prostate	12		15.3	1.03	15.8
81	Left Breast	25	235.9		0.94	222
82	Right Breast	25	235.9		0.94	222
81	Left Breast	25		81.1	0.94	76.2
82	Right Breast	25		81.1	0.94	76.2

Additionally, for completeness, lymph nodes are specified as cells 142-147.

7.2 Animal Phantoms

The generalized animal phantom is shown in Figure 7-8. This provides locations of various cells (organs) as listed in

Table 7-9. The phantom is scaled by mass (Section 7.3) from a small cat, through the dog, to a large horse to maintain the general placement of organs. Animal phantoms differ in snout size, neck length, thyroid placement, and leg length, but are otherwise based on the same general model.

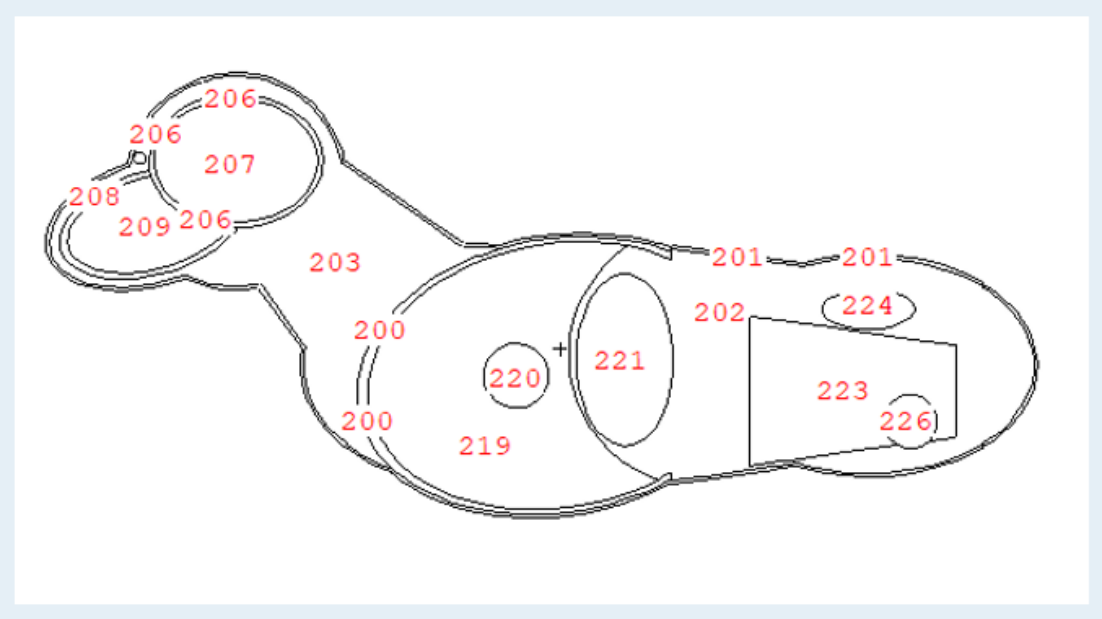

Figure 7-8 2D Center-Line Cross Section of Companion Animal.

Table 7-9 Animal Parameter Values of Volume, Density, and Mass.

Cell	Component	Material	Volume (cm^3)	Density (g/cm^3)	Mass (g)
200	Ribs	2	1649	1.4	2310
201	Skin	11	4400	1.09	4800
202	Abdominal Space	12	5562	1.03	5730
203	Neck	12	1800	1.03	1850
204	Spine	2	1455	1.4	2040
205	Thyroid	10	30	1.05	31.5
206	Skull	2	249	1.4	349
207	Brain	6	1128	1.04	1170
208	Face	12	1500	1.03	1550
209	Jaw	2	369	1.4	517
210	Eyes	7	8.4	1.07	8.99
211	L Humerus	2	102	1.4	143
212	L Scapula	2	102	1.4	143
213	L Bony Forelimb	2	14	1.4	19.6
236		2	100	1.4	140
237		2	14	1.4	19.6
238		2	77	1.4	108
214	L ST Forelimb	13	134	1.05	141
239		13	19	1.05	20.0
240		13	103	1.05	108
241		13	19	1.05	19.95
215	R Humerus	2	102	1.4	142.8
216	R Scapula	2	102	1.4	142.8

Table 7-9 Animal Parameter Values of Volume, Density, and Mass (Cont.).

Cell	Component	Material	Volume (cm^3)	Density (g/cm^3)	Mass (g)
217	R Bony Forelimb	2	14	1.4	19.6
242		2	100	1.4	140
243		2	14	1.4	19.6
244		2	77	1.4	108
218	R ST Forelimb	13	134	1.05	141
245		13	19	1.05	20.0
246		13	103	1.05	108
247		13	19	1.05	20.0
219	Lungs	14	2500	0.26	650
220	Heart	15	375	1.05	394
221	Liver	17	1000	1.05	1050
222	Stomach	20	1000	1.03	1030
223	Intestines	20	2000	1.03	2060
224	Kidneys	16	255	1.05	268
226	Urinary Bladder	21	300	1.04	312
227	Uterus	24	300	1.02	306

Table 7-9 Animal Parameter Values of Volume, Density, and Mass (Cont.).

Cell	Component	Material	Volume (cm^3)	Density (g/cm^3)	Mass (g)
228	R femur	2	106	1.4	148
229	R pelvic Hemisphere	2	87	1.4	122
230	R femur	2	14	1.4	19.6
248	R pelvic Hemisphere	2	111	1.4	155
249		2	14	1.4	19.6
250		2	77	1.4	108
231		13	22	1.05	23.1
251		13	175	1.05	184
252		13	22	1.05	23.1
253	R ST Hindlimb	13	121	1.05	127
232	L femur	2	106	1.4	148
233	L Pelvic Hemisphere	2	87	1.4	122
234	L Bony Hindlimb	2	14	1.4	19.6
254		2	111	1.4	155
255		2	14	1.4	19.6
256		2	77	1.4	108
235		13	22	1.05	23.1
257		13	175	1.05	184
258		13	22	1.05	23.1
259	L ST Hindlimb	13	121	1.05	127

7.3 Animal Scaling

PiMAL 6.0 allows the user to select cat, dog, or horse and then specify the mass of the animal. These selections build a scaled volume representing total mass of that animal type. Generally, the volume parameters correspond mathematically with the computed volume in expected geometric ways that follow an approximate third power rule (Figure 7-9 and Figure 7-10). The relationship was developed by aggregating data from various

sources on cat, dog, and horse conformation (Zink 2020; Serpell 2017; Ross 2017; Duberstein 2016; Jörg 2019).

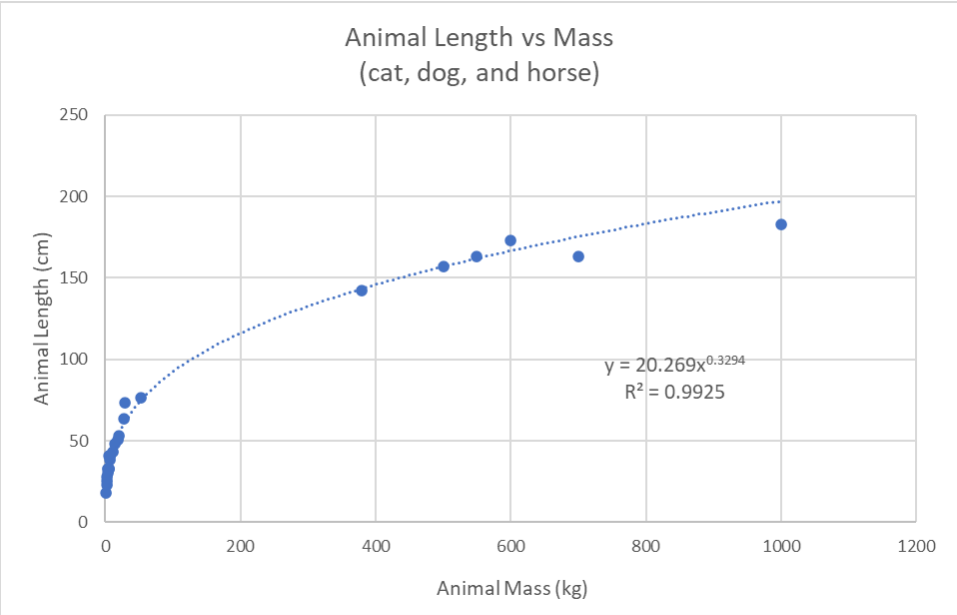

Figure 7-9 Animal Length as a Function of Animal Mass.

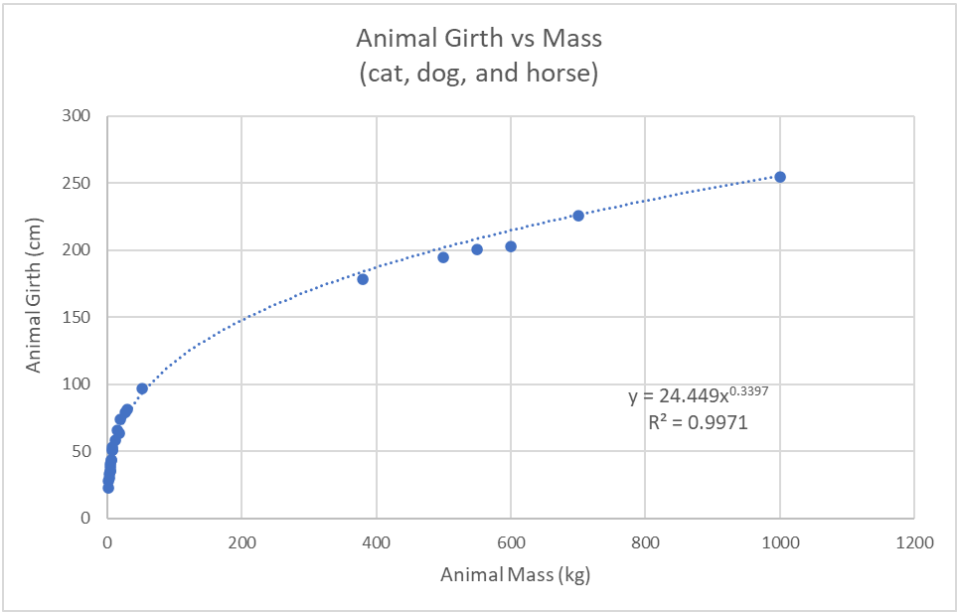

Figure 7-10 Animal Girth as a Function of Animal Mass.

The parameters for the curve fit show that the relationship between mass and length (as well as mass and girth) maintains a similar power function. The animal length vs mass relationship ($length = 20.3 * mass^{0.329}$) was used to scale the companion animal from 0.5 kg through 1,500 kg. Because the volumes in the MCNP file are generated based on

intersections of various geometric shapes (i.e., radii are not defined for the body length, rather as sections with a total of a specified length), the relationship above is applied as a ratio rather than to solve for individual volume lengths. For example, the total body length corresponding to a 30 kg animal is 62.2 cm:

$$L(30\ kg) = 20.3 * 30^{0.329} = 62.2\ cm \quad [7.1]$$

This is used as the baseline length to scale all other length parameters in the MCNP file. Given that the total length of a 40 kg animal is,

$$L(40\ kg) = 20.3 * 40^{0.329} = 68.3\ cm \quad [7.2]$$

the proportion of this to the baseline is 68.3/62.2 = 1.10. Similarly, a 10 kg animal would have a total length of,

$$L(10\ kg) = 20.3 * 10^{0.329} = 43.3\ cm \quad [7.3]$$

corresponding to a proportion of 0.696. This ratio, for example, is applied to all length parameters in the MCNP base file to scale the animal's length according to the mass input. Using this technique, each of the internal organs will retain body mass ratio of each animal. Morphometrics generally suggests that critical organs follow a proportionality with the total mass of the animal; for example, a liver is generally about 2.2 percent of the total body mass (Ross 2018). For this reason, scaling the animal by total mass will generally retain an accurate representation of the mass, and thus volume, of each animal organ.

Because there is ***inter***-species variation between PiMAL animals in the limb, neck and head/face parameters, simple scaling between the three animals for these parameters is not appropriate. The user, therefore, selects the appropriate animal and the resulting phantom will reflect these variations. Since the differences in scaling between animals is limited to skeletal features (i.e., legs, neck, face), all organ volumes representing sources used for radiation dose calculations are excluded from this interspecies variation, but the locations of the organs will be more accurate based on the height of the animal.

Given the large ***intra***-species variation for each of the PiMAL animals, no phantom will be exactly representative of any particular companion animal. However, as a general rule (Zink and Schlehr 2020; Duberstein 2016) both dogs and horses are square in that the length of the body is equal to the height of the animal at the withers, and that both dogs and horses have leg lengths that are approximately equal to one-half their height (Figure 7-11). The values used to calculate the base line proportion discrepancies for the three listed species were found using the information in horse and dog conformation references (Zink and Schlehr 2020; Duberstein 2016) and cat-breed size estimates. Neck lengths for

horses are found in conformation references, and the length of the dog's neck has been scaled from baseline spine-length measurements of 30 kg dogs (Miller 2012).

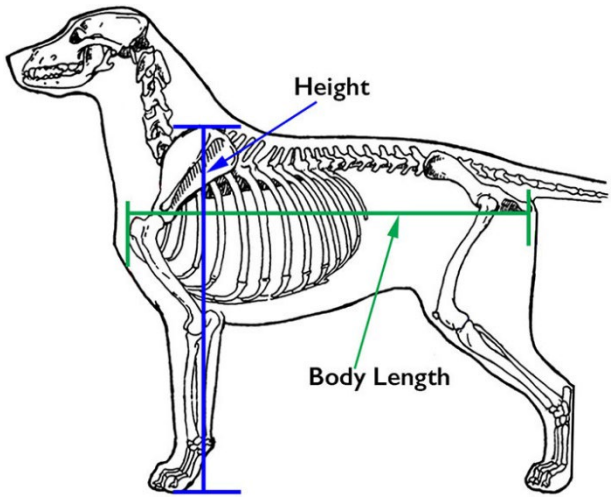

Figure 7-11 Demonstration of Body Length and Height Relationship.

There is a difference, however, in horse and dog location of the knee joint (Zink 2020; Mostafa 2020). For this reason, an average is set to represent the likely location of important joints (in the dog and horse, the knee joint is a critical source location for radiotherapy treatments), and in the case of the dog, skews the square body rule slightly for that critical anatomical feature to be represented in the animal. Table 7-10 provides specific scaling factors in the face, neck, and limbs of the three animals phantoms.

Table 7-10 Data Used to Relate Skeletal Differences Between Animal Phantoms.

	Cat	Dog	Horse
Face	sphere	ovoid	ovoid
	1% Spine Length	20% Spine length	33% neck length
Neck	20% Spine Length	30% spine length	50% spine length
Lower Leg	50% upper leg	90% upper leg	100% upper leg
Upper leg	25% spine length	25% spine length	25% spine length
Height	60% spine Length	100% Spine Length	100% Spine Length

It is important to note that these values are approximations based on horse, dog and cat conformation and body size distributions, and not representative of a particular breed or size of animal. The location of major organs and ratios of those organs to the mass of the animal are maintained so that volumes and locations can be preserved based on the mass of the animal alone, and do not need to be modified from one animal phantom to the other. In the same way, the elemental composition and density of the organs

themselves are maintained through all species (companion animals and humans) to maintain MCNP phantom compatibility.

8 STANDARD POSITIONAL RELATIONSHIPS

With v6.0, PiMAL has the capability of pairing a human and animal in the same Monte Carlo universe. This allows the user to model the radiation dose to humans from medically applied radioactivity in a companion animal (i.e., cat, dog, horse). For this pairing, only one human and one animal can be in the same universe. Various relationships between human and animal phantoms have been developed to assist the user in a quick initial positioning (Table 8-1 through Table 8-6). The human is always centered on (0, 0, 0) and the animal is moved in relation to the human.

8.1 Cat Placement

8.1.1 Cat in the Lap of a Human Female

Table 8-1 5 kg Cat Placement with Respect to the Human Female.

Human Female	Articulation	placement	5 kg Cat	Location/Joint	placement
R Shoulder	X Rotation	0	Base	X Location	-9
	Y Rotation	0		Y Location	-25
R Elbow	X Rotation	0		Z Location	17
	Y Rotation	0		Z Rotation	0
L Shoulder	X Rotation	0	L Fore Knee	Y Rotation	-40
	Y Rotation	0	L Fore Ankle	Y Rotation	150
L Elbow	X Rotation	0	R Fore Knee	Y Rotation	-40
	Y Rotation	0	R Fore Ankle	Y Rotation	150
R Hip	X Rotation	-80	L Hind Knee	Y Rotation	-40
	Y Rotation	0	L Hind Ankle	Y Rotation	125
R Knee	X Rotation	90	R Hind Knee	Y Rotation	-40
	Y Rotation	0	R Hind Ankle	Y Rotation	125
L Hip	X Rotation	-80			
	Y Rotation	0			
L Knee	X Rotation	90			
	Y Rotation	0			

8.1.2 Cat sleeping on the chest of a Human Male

Table 8-2 3 kg Cat Placement with Respect to the Human Male.

5 kg Cat	Location/Joint	on chest
Base	X Location	5
	Y Location	-20
	Z Location	45
	Z Rotation	0

8.2 Dog Placement

8.2.1 Dog at the Feet and Walking with Human Male

Table 8-3 30 kg Dog Placement with Respect to the Human Male.

Location	Articulation	at the feet	walking beside
Base	X Location	5	40
	Y Location	-25	10
	Z Location	-28	-28
	Z Rotation	0	90

8.2.2 Dog in the Lap of a Human

Table 8-4 10 kg Dog Placement with Respect to the Human Female.

Human Female	Articulation	placement	10 kg Dog	Location/Joint	placement
R Shoulder	X Rotation	0	Base	X Location	-9
	Y Rotation	0		Y Location	-25
R Elbow	X Rotation	0		Z Location	21
	Y Rotation	0		Z Rotation	0
L Shoulder	X Rotation	0	L Fore Knee	Y Rotation	-40
	Y Rotation	0	L Fore Ankle	Y Rotation	150
L Elbow	X Rotation	0	R Fore Knee	Y Rotation	-40
	Y Rotation	0	R Fore Ankle	Y Rotation	150
R Hip	X Rotation	-80	L Hind Knee	Y Rotation	-40
	Y Rotation	0	L Hind Ankle	Y Rotation	125
R Knee	X Rotation	90	R Hind Knee	Y Rotation	-40
	Y Rotation	0	R Hind Ankle	Y Rotation	125
L Hip	X Rotation	-80			
	Y Rotation	0			
L Knee	X Rotation	90			
	Y Rotation	0			

8.3 Horse Placement

8.3.1 Human Grooming and Leading a Horse

Table 8-5 300 kg Horse Placement with Respect to the Human Female.

Location	Articulation	grooming	leading
Base	X Location	10	0
	Y Location	-65	200
	Z Location	30	30
	Z Rotation	0	90

8.3.2 Human Riding a Horse

Table 8-6 Human Female Placement with Respect to 300 kg Horse.

Human Female	Articulation	placement	300 kg Horse	Location/Joint	placement
R Shoulder	X Rotation	-30	Base	X Location	0
	Y Rotation	0		Y Location	-15
R Elbow	X Rotation	-30		Z Location	-45
	Y Rotation	0		Z Rotation	90
L Shoulder	X Rotation	-30	L Fore Knee	Y Rotation	0
	Y Rotation	0	L Fore Ankle	Y Rotation	0
L Elbow	X Rotation	-30	R Fore Knee	Y Rotation	0
	Y Rotation	0	R Fore Ankle	Y Rotation	0
R Hip	X Rotation	-60	L Hind Knee	Y Rotation	0
	Y Rotation	50	L Hind Ankle	Y Rotation	0
R Knee	X Rotation	60	R Hind Knee	Y Rotation	0
	Y Rotation	0	R Hind Ankle	Y Rotation	0
L Hip	X Rotation	-60			
	Y Rotation	-50			
L Knee	X Rotation	60			
	Y Rotation	0			

9 BENCHMARKING THE EFFECTIVE DOSE CALCULATION

The effective dose (using ICRP 60 tissue weighting factors) to a female is calculated for an exposure of 1.5 hours (τ) at 1.5 meters from the chest to a 1 GBq (A_0), Sn-117m point source (Figure 9-1). The source is external to the body (i.e., no biological loss), therefore the effective loss constant (λ_e) only considers physical decay and has a value of 5.90E-07 [s^{-1}] (half-life of 13.6 days).

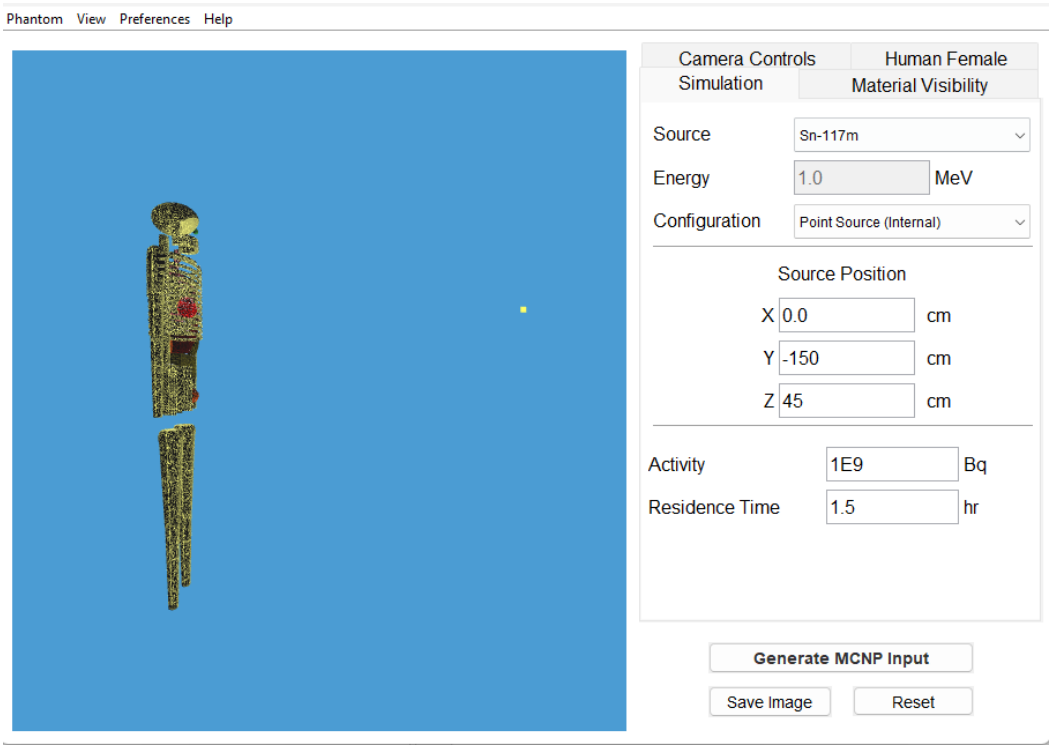

Figure 9-1 Simulation Panel Showing Location of the Sn-117m Point Source.

The total number of transitions ($\tilde{A}$) occurring during the 1.5-hour exposure is equal to:

$$\tilde{A} = 1x10^{9}\left(\frac{1-e^{-(5.90x10^{-7}*5400)}}{5.90x10^{-7}\ [s^{-1}]}\right) = 5.39x10^{12}\ [nt] \qquad [9.1]$$

With one-million simulated particles, an MCNP F6 output of 1.32x10^{-8} [MeV/g γ] for the thyroid, a radiation weighting factor (w_r) of 1 [Sv/Gy], and a probability of photon emission (P) of 1.552 [γ/nt], the thyroid organ equivalent dose (H_i) is:

$$H_i = 1.32x10^{-8}\left[\frac{MeV}{g\,\gamma}\right] * 1\left[\frac{Sv}{Gy}\right] * 5.39x10^{12}[nt] * 1.552\left[{}^{\gamma}/_{nt}\right] * 1.602x10^{-10}\left[\frac{J\,g}{MeV\,kg}\right] = 1.77x10^{-5}\,[Sv] \quad [9.2]$$

With effective dose calculated the ICRP 60 (1991) list of organs and the five highest remainder organs, the effective dose can be estimated. The effective dose (E) is the sum of all organ-specific equivalent dose (H_i) multiplied by their respective tissue weight factor. As an example, PiMAL reports organ absorbed dose per source photon (F6 tally) as shown in Table 9-1 with an effective dose calculation using the ICRP 60 method.

Table 9-1 Pertinent Data from ICRP 60.

Organ, *i*	$w_{T,i}$	$F6_i$ (MeV/g γ)	H_i * $w_{T,i}$ (Sv)
Bladder	0.05	1.51E-08	1.01E-06
Bone Marrow	0.12	1.17E-08	1.88E-06
Bone Surface	0.01	1.73E-08	2.32E-07
Breast	0.05	1.85E-08	1.24E-06
Colon	0.12	1.01E-08	1.62E-06
Esophagus	0.05	6.93E-09	4.64E-07
Ovaries	0.20	1.21E-08	3.24E-06
Liver	0.05	1.21E-08	8.11E-07
Lung	0.12	1.01E-08	1.11E-06
Skin	0.01	1.75E-08	2.35E-07
Stomach	0.12	1.23E-08	1.98E-06
Thyroid	0.05	1.32E-08	8.85E-07
Remainder*	0.05	8.65E-09	6.44E-08
Effective Dose		**E (Sv) =**	**1.58E-05**

*average of the nine named (Table 6-2) remainder organ doses

The effective dose estimated above is 1.58x10^{-5} Sv, starting with the various F6 tallies and following through with a hand calculation. The PiMAL code calculates the effective dose to be 1.61E^{-5} Sv (Figure 9-2).

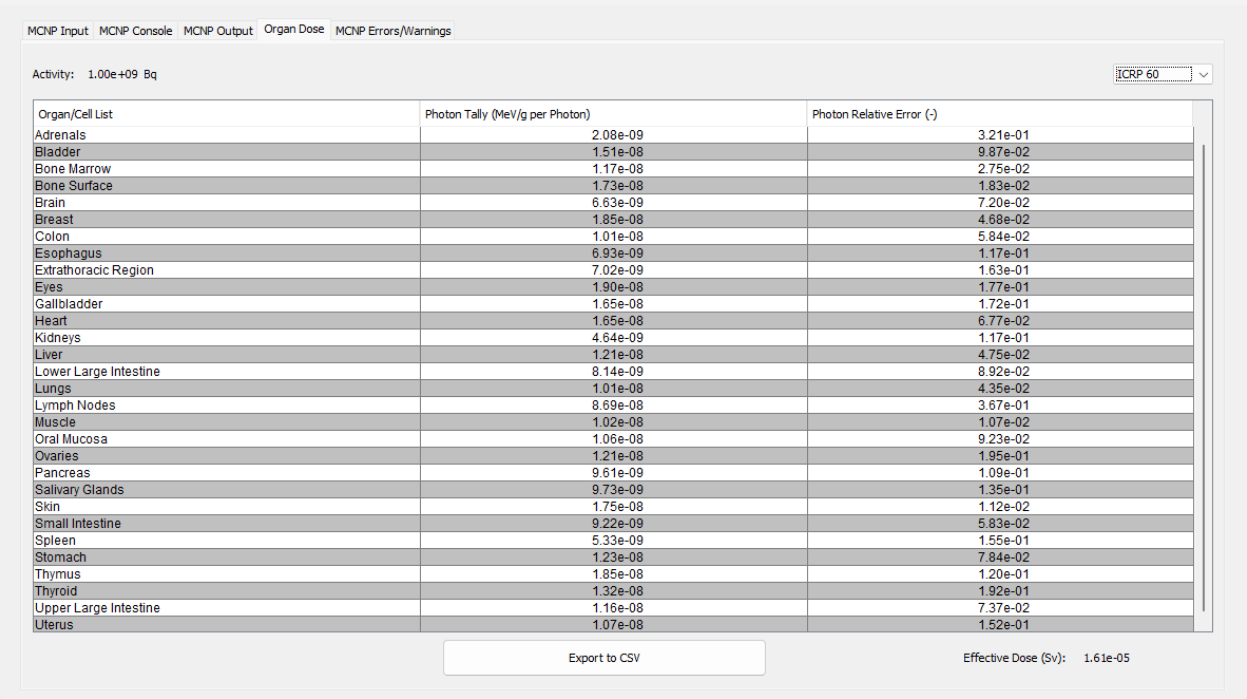

Organ/Cell List	Photon Tally (MeV/g per Photon)	Photon Relative Error (-)
Adrenals	2.08e-09	3.21e-01
Bladder	1.51e-08	9.87e-02
Bone Marrow	1.17e-08	2.75e-02
Bone Surface	1.73e-08	1.83e-02
Brain	6.63e-09	7.20e-02
Breast	1.85e-08	4.68e-02
Colon	1.01e-08	5.84e-02
Esophagus	6.93e-09	1.17e-01
Extrathoracic Region	7.02e-09	1.63e-01
Eyes	1.90e-08	1.77e-01
Gallbladder	1.65e-08	1.72e-01
Heart	1.65e-08	6.77e-02
Kidneys	4.64e-09	1.17e-01
Liver	1.21e-08	4.75e-02
Lower Large Intestine	8.14e-09	8.92e-02
Lungs	1.01e-08	4.35e-02
Lymph Nodes	8.69e-08	3.67e-01
Muscle	1.02e-08	1.07e-02
Oral Mucosa	1.06e-08	9.23e-02
Ovaries	1.21e-08	1.95e-01
Pancreas	9.61e-09	1.09e-01
Salivary Glands	9.73e-09	1.35e-01
Skin	1.75e-08	1.12e-02
Small Intestine	9.22e-09	5.83e-02
Spleen	5.33e-09	1.55e-01
Stomach	1.23e-08	7.84e-02
Thymus	1.85e-08	1.20e-01
Thyroid	1.32e-08	1.92e-01
Upper Large Intestine	1.16e-08	7.37e-02
Uterus	1.07e-08	1.52e-01

Figure 9-2 Organ Dose Output Window for the ICRP 60 EDE Methodology.

10 REFERENCES

Akkurt, H.; Eckerman, K.F. "Development of PIMAL: Mathematical Phantom with Moving Arms and Legs". Oak Ridge National Laboratory. Report No. ORNL/TM-2007/14. Oak Ridge, TN: 2007.

Bushong, S.C. Radiological Science for Technologists: Physics, Biology, and Protection. 9th ed. 2008. Mosby Elsevier. St. Louis, MO.

Duberstein, K.J. Horse Conformation. https://extension.uga.edu/publications. Bulletin 1400. 2016.

Evans, H.E.; de Lahunta, A. Miller's Anatomy of the Dog. Saunders. https://books.google.com/books?id=6eBOAQAAQBAJ. 2012.

ICRP, 1977. Recommendations of the ICRP. ICRP Publication 26. Ann. ICRP 1 (3).

ICRP, 1991. 1990 Recommendations of the International Commission on Radiological Protection. ICRP Publication 60. Ann. ICRP 21 (1-3).

ICRP, 1996. Conversion Coefficients for use in Radiological Protection Against External Radiation. ICRP Publication 74. Ann. ICRP 26 (3-4).

ICRP, 2002. Basic Anatomical and Physiological Data for Use in Radiological Protection Reference Values. ICRP Publication 89. Ann. ICRP 32 (3-4).

ICRP, 2007. The 2007 Recommendations of the International Commission on Radiological Protection. ICRP Publication 103. Ann. ICRP 37 (2-4).

ICRP, 2009. Adult Reference Computational Phantoms. ICRP Publication 110. Ann. ICRP 39 (2).

Jörg A. A.; Stick, J.A.; Kümmerle, J.M.; Prange, T. *Equine Surgery (Fifth Edition)*. W.B. Saunders. ISBN 9780323484206, https://doi.org/10.1016/B978-0-323-48420-6.00111-3. 2019.

Mostafa, M.B.; Elemmawy, Y.M. Relationships between morphometric measurements and musculoskeletal disorders in jumping thoroughbred horses. *J Equine Sci*. Jun;31(**2**):23-27. https://10.1294/jes.31.23. PMID: 32617072; PMCID: PMC7316700. 2020.

Pelowitz, D.B.; Goorley, J.T.; James, M.R.; et al. MCNP6 User's Manual. Los Alamos National Laboratory. Technical Report No. LA-CP-13-00634. Los Alamos, NM: May 2013.

Radiopaedia.org. access date 11/19/2024. https://radiopaedia.org/cases/energy-spectrum-of-tungsten-anode-at-80kvp-and-100-kvp

Ross, T. Necropsy Guide for Dogs, Cats and Small Mammals. SP McDonough and T. Southward (eds). Wiley Blackwell. ISBN 9781119115656. *Australian Veterinary Journal*. 96. 38-38. https://10.1111/avj.12665. 2017.

Serpell, J. The Domestic Dog: Its Evolution, Behavior and Interactions with People. Cambridge, United Kingdom, Cambridge University Press. 2017.

Xu, X.G. An exponential growth of computational phantom research in radiation protection, imaging, and radiotherapy: A review of the fifty-year history. *Physics in Medicine and Biology*. 59(**18**): 2014.

Zink, C.; Schlehr, M.R. Working dog structure: Evaluation and relationship to function. *Frontiers in Veterinary Science*. 7:559055. https://10.3389/fvets.2020.559055. 2020.

Appendix A MCNP Source Data

Nuclide emissions data are from ICRP 107 with yield greater than 1% and energy greater than 10 keV.

4.17E-09 inv sec

C ===== Co-60 Energies

SI10 L 1.17323 1.33249

C ===== Co-60 Probabilities

SP10 D 0.999 1.000

1.06E-08 inv sec

C ===== Cs-134 Energies

SI10 L 0.475365 0.563246 0.569331 0.604721

0.795864 0.801953 1.167970 1.365190

C ===== Cs-134 Probabilities

SP10 D 0.0149 0.0835 0.1540 0.9760

0.8550 0.0869 0.0179 0.0301

7.28E-10 inv sec

C ===== Cs-137 Energies

SI10 L 0.0318187 0.0322056 0.0363167 0.036392 0.0372607 0.661657

C ===== Cs-137 Probabilities

SP10 D 0.0204 0.0375 0.00358 0.00694 0.00148 0.846

1.09E-07 inv sec

C ===== Ir-192 Energies

SI10 L 0.011101 0.061642 0.063189 0.065302 0.067048

0.205794 0.295957 0.308455 0.316506 0.468069 0.484575

0.588581 0.604411 0.612462

C ===== Ir-192 Probabilities

SP10 D 0.0135 0.0124 0.0213 0.0268 0.0458

0.0334 0.2870 0.2970 0.8270 0.4780 0.0319

0.0452 0.0820 0.0534

1.00E-07 inv sec

C ===== I-131 Energies

SI10 L 0.029452 0.029781 0.080185 0.284305 0.364489 0.636989 0.722911

C ===== I-131 Probabilities

SP10 D 0.0140 0.0259 0.0262 0.0614 0.817 0.0717 0.0177

1.21E-06 inv sec

C ===== Lu-177 Energies

SI10 L 0.054719 0.055924 0.112950 0.208366

C ===== Lu-177 Probabilities

SP10 D 0.0163 0.0285 0.0640 0.1100

5.90e-07 inv sec

C ===== Sn-117m Energies

SI10 L 0.025023 0.025257 0.028431 0.028474

0.029088 0.156020 0.158560

C ===== Sn-117m Probabilities

SP10 D 0.1940 0.3630 0.0328 0.0636

0.0131 0.0211 0.8640

C ==== XRay Tube Voltage 60 kVp, Source Energies

SI10 H 0.0125 0.0130 0.0135 0.0140 0.0145 0.0150

0.0155 0.0160 0.0165 0.0170 0.0175 0.0180

0.0185 0.0190 0.0195 0.0200 0.0205 0.0210

0.0215 0.0220 0.0225 0.0230 0.0235 0.0240

0.0245 0.0250 0.0255 0.0260 0.0265 0.0270

0.0275 0.0280 0.0285 0.0290 0.0295 0.0300

0.0305 0.0310 0.0315 0.0320 0.0325 0.0330

0.0335 0.0340 0.0345 0.0350 0.0355 0.0360

0.0365 0.0370 0.0375 0.0380 0.0385 0.0390

0.0395 0.0400 0.0405 0.0410 0.0415 0.0420

0.0425 0.0430 0.0435 0.0440 0.0445 0.0450

0.0455 0.0460 0.0465 0.0470 0.0475 0.0480

0.0485 0.0490 0.0495 0.0500 0.0505 0.0510

0.0515 0.0520 0.0525 0.0530 0.0535 0.0540

0.0545 0.0550 0.0555 0.0560 0.0565 0.0570

0.0575 0.0580 0.0585 0.0590 0.0595 0.0600

C ==== XRay Tube Voltage 60 kVp, Source Probabilities

SP10 D 0.0000 0.0000 0.0001 0.0003 0.0007 0.0016

0.0033 0.0062 0.0108 0.0179 0.0277 0.0409

0.0580 0.0790 0.1045 0.1338 0.1662 0.2041

0.2432 0.2864 0.3304 0.3771 0.4216 0.4709

0.5154 0.5583 0.6041 0.6469 0.6857 0.7259

0.7611 0.7975 0.8272 0.8576 0.8802 0.903

0.9260 0.9402 0.9579 0.9698 0.9808 0.9887

0.9942 0.9976 1.0000 0.9988 0.9973 0.9936

0.9875 0.9810 0.9724 0.9634 0.9525 0.9402

0.9275 0.9136 0.8985 0.8824 0.8651 0.8477

0.8299 0.8105 0.7917 0.7711 0.7508 0.7293

0.7081 0.6861 0.6632 0.6411 0.6179 0.5942

0.5711 0.5472 0.5227 0.4987 0.4741 0.4495

0.4249 0.3998 0.3751 0.3500 0.3249 0.2998

0.2745 0.2494 0.2241 0.1989 0.1738 0.1488

0.1238 0.0988 0.0739 0.0492 0.0245 0.0020

C ==== XRay Tube Voltage 80 kVp, Source Energies

SI10 H 0.0130 0.0135 0.0140 0.0145 0.0150 0.0155
0.0160 0.0165 0.0170 0.0175 0.0180 0.0185 0.0190
0.0195 0.0200 0.0205 0.0210 0.0215 0.0220 0.0225
0.0230 0.0235 0.0240 0.0245 0.0250 0.0255 0.0260
0.0265 0.0270 0.0275 0.0280 0.0285 0.0290 0.0295
0.0300 0.0305 0.0310 0.0315 0.0320 0.0325 0.0330
0.0335 0.0340 0.0345 0.0350 0.0355 0.0360 0.0365
0.0370 0.0375 0.0380 0.0385 0.0390 0.0395 0.0400
0.0405 0.0410 0.0415 0.0420 0.0425 0.0430 0.0435
0.0440 0.0445 0.0450 0.0455 0.0460 0.0465 0.0470
0.0475 0.0480 0.0485 0.0490 0.0495 0.0500 0.0505
0.0510 0.0515 0.0520 0.0525 0.0530 0.0535 0.0540
0.0545 0.0550 0.0555 0.0560 0.0565 0.0570 0.0575
0.0580 0.0585 0.0590 0.0595 0.0600 0.0605 0.0610
0.0615 0.0620 0.0625 0.0630 0.0635 0.0640 0.0645
0.0650 0.0655 0.0660 0.0665 0.0670 0.0675 0.0680
0.0685 0.0690 0.0695 0.0700 0.0705 0.0710 0.0715
0.0720 0.0725 0.0730 0.0735 0.0740 0.0745 0.0750
0.0755 0.0760 0.0765 0.0770 0.0775 0.0780 0.0785
0.0790 0.0795 0.0800

C ==== XRay Tube Voltage 80 kVp, Source Probabilities

SP10 D 0.0000 0.0000 0.0001 0.0003 0.0007 0.0015

0.0028 0.0050 0.0083 0.0131 0.0197 0.0284 0.0394

0.0531 0.0693 0.0877 0.1096 0.1329 0.1593 0.1868

0.2167 0.2461 0.2790 0.3098 0.3403 0.3732 0.4048

0.4345 0.4655 0.4938 0.5231 0.5485 0.5746 0.5958

0.6173 0.6392 0.6551 0.6737 0.6883 0.7024 0.7144

0.7249 0.7339 0.7422 0.7480 0.7537 0.7578 0.7601

0.7623 0.7630 0.7635 0.7626 0.7607 0.7587 0.7557

0.7519 0.7474 0.7421 0.7367 0.7312 0.7244 0.7183

0.7107 0.7036 0.6954 0.6877 0.6794 0.6702 0.6621

0.6530 0.6435 0.6347 0.6252 0.6151 0.6056 0.5957

0.5857 0.5758 0.5654 0.5556 0.5452 0.5350 0.5247

0.5140 0.5039 0.4933 0.4827 0.4722 0.4618 0.4514

0.7769 0.4302 0.4199 1.0000 0.3987 0.3881 0.3776

0.3672 0.3567 0.3464 0.3357 0.3254 0.3151 0.3046

0.2941 0.2839 0.2736 0.2632 0.4525 0.2427 0.2325

0.2223 0.2650 0.2005 0.1829 0.1739 0.1648 0.1558

0.1467 0.1375 0.1284 0.1191 0.1100 0.1008 0.0916

0.0824 0.0732 0.0640 0.0548 0.0456 0.0365 0.0273

0.0182 0.0091 0.0008

C ==== XRay Tube Voltage 100 kVp, Source Energies

SI10 H 0.0135 0.0140 0.0145 0.0150 0.0155 0.0160 0.0165

0.0170 0.0175 0.0180 0.0185 0.0190 0.0195 0.0200

0.0205 0.0210 0.0215 0.0220 0.0225 0.0230 0.0235

0.0240 0.0245 0.0250 0.0255 0.0260 0.0265 0.0270

0.0275 0.0280 0.0285 0.0290 0.0295 0.0300 0.0305

0.0310 0.0315 0.0320 0.0325 0.0330 0.0335 0.0340

0.0345 0.0350 0.0355 0.0360 0.0365 0.0370 0.0375

0.0380 0.0385 0.0390 0.0395 0.0400 0.0405 0.0410

0.0415 0.0420 0.0425 0.0430 0.0435 0.0440 0.0445

0.0450 0.0455 0.0460 0.0465 0.0470 0.0475 0.0480

0.0485 0.0490 0.0495 0.0500 0.0505 0.0510 0.0515

0.0520 0.0525 0.0530 0.0535 0.0540 0.0545 0.0550

0.0555 0.0560 0.0565 0.0570 0.0575 0.0580 0.0585

0.0590 0.0595 0.0600 0.0605 0.0610 0.0615 0.0620

0.0625 0.0630 0.0635 0.0640 0.0645 0.0650 0.0655

0.0660 0.0665 0.0670 0.0675 0.0680 0.0685 0.0690

0.0695 0.0700 0.0705 0.0710 0.0715 0.0720 0.0725

0.0730 0.0735 0.0740 0.0745 0.0750 0.0755 0.0760

0.0765 0.0770 0.0775 0.0780 0.0785 0.0790 0.0795

0.0835 0.0840 0.0845 0.0850 0.0855 0.0860 0.0865

0.0870 0.0875 0.0880 0.0885 0.0890 0.0895 0.0900

0.0905 0.0910 0.0915 0.0920 0.0925 0.0930 0.0935

0.0940 0.0950 0.0955 0.0960 0.0965 0.0970 0.0975

0.0980 0.0985 0.0990 0.0995 0.1000

C ==== XRay Tube Voltage 100 kVp, Source Probabilities

SP10 D 0.0000 0.0000 0.0001 0.0002 0.0003 0.0006

0.0012 0.0020 0.0031 0.0047 0.0069 0.0096 0.0131

0.0172 0.0221 0.0279 0.0343 0.0416 0.0494 0.0580

0.0668 0.0766 0.0862 0.0958 0.1063 0.1167 0.1266

0.1372 0.1470 0.1574 0.1666 0.1762 0.1844 0.1928

0.2013 0.2080 0.2156 0.2220 0.2282 0.2338 0.2388

0.2434 0.2477 0.2512 0.2546 0.2575 0.2597 0.2619

0.2636 0.2651 0.2661 0.2668 0.2674 0.2676 0.2675

0.2672 0.2665 0.2658 0.2650 0.2638 0.2628 0.2612

0.2597 0.2579 0.2563 0.2543 0.2521 0.2503 0.2480

0.2457 0.2435 0.2412 0.2386 0.2362 0.2336 0.2311

0.2285 0.2258 0.2233 0.2206 0.2179 0.2152 0.2124

0.2098 0.2070 0.2042 0.2015 0.1988 0.1961 0.6539

0.1906 0.1879 1.0000 0.1824 0.1797 0.1770 0.1743

0.1716 0.1690 0.1662 0.1636 0.1611 0.1584 0.1557

0.1532 0.1505 0.1479 0.4285 0.1427 0.1402 0.1377

0.2105 0.1294 0.1114 0.1098 0.1081 0.1065 0.1049

0.1031 0.1015 0.0997 0.0980 0.0963 0.0946 0.0928

0.0782 0.0763 0.0745 0.0726 0.0707 0.0689 0.0670

0.0651 0.0631 0.0612 0.0593 0.0574 0.0554 0.0535

0.0516 0.0497 0.0478 0.0458 0.0439 0.0419 0.0400

0.0381 0.0361 0.0342 0.0323 0.0303 0.0284 0.0265

0.0246 0.0226 0.0188 0.0169 0.0150 0.0131 0.0112

0.0093 0.0075 0.0056 0.0037 0.0019 0.0001

C ==== XRay Tube Voltage 120 kVp, Source Energies

SI10 H 0.0140 0.0145 0.0150 0.0155 0.0160 0.0165 0.0170

0.0175 0.0180 0.0185 0.0190 0.0195 0.0200 0.0205

0.0210 0.0215 0.0220 0.0225 0.0230 0.0235 0.0240

0.0245 0.0250 0.0255 0.0260 0.0265 0.0270 0.0275

0.0280 0.0285 0.0290 0.0295 0.0300 0.0305 0.0310

0.0315 0.0320 0.0325 0.0330 0.0335 0.0340 0.0345

0.0350 0.0355 0.0360 0.0365 0.0370 0.0375 0.0380

0.0385 0.0390 0.0395 0.0400 0.0405 0.0410 0.0415

0.0420 0.0425 0.0430 0.0435 0.0440 0.0445 0.0450

0.0455 0.0460 0.0465 0.0470 0.0475 0.0480 0.0485

0.0490 0.0495 0.0500 0.0505 0.0510 0.0515 0.0520

0.0525 0.0530 0.0535 0.0540 0.0545 0.0550 0.0555

0.0560 0.0565 0.0570 0.0575 0.0580 0.0585 0.0590

0.0595 0.0600 0.0605 0.0610 0.0615 0.0620 0.0625

0.0630 0.0635 0.0640 0.0645 0.0650 0.0655 0.0660

0.0665 0.0670 0.0675 0.0680 0.0685 0.0690 0.0695

0.0700 0.0705 0.0710 0.0715 0.0720 0.0725 0.0730

0.0735 0.0740 0.0745 0.0750 0.0755 0.0760 0.0765

0.0770 0.0775 0.0780 0.0785 0.0790 0.0795 0.0800

0.0805 0.0810 0.0815 0.0820 0.0825 0.0830 0.0835

0.0840 0.0845 0.0850 0.0855 0.0860 0.0865 0.0870

0.0875 0.0880 0.0885 0.0890 0.0895 0.0900 0.0905

0.0910 0.0915 0.0920 0.0925 0.0930 0.0935 0.0940

0.0945 0.0950 0.0955 0.0960 0.0965 0.0970 0.0975

0.0980 0.0985 0.0990 0.0995 0.1000 0.1005 0.1010

0.1015 0.1020 0.1025 0.1030 0.1035 0.1040 0.1045

0.1050 0.1055 0.1060 0.1065 0.1070 0.1075 0.1080

0.1085 0.1090 0.1095 0.1100 0.1105 0.1110 0.1115

0.1120 0.1125 0.1130 0.1135 0.1140 0.1145 0.1150

0.1155 0.1160 0.1165 0.1170 0.1175 0.1180 0.1185

0.1190 0.1195 0.1200

C ==== XRay Tube Voltage 120 kVp, Source Probabilities

SP10 D 0.0000 0.0000 0.0001 0.0002 0.0003 0.0005 0.0009

0.0014 0.0022 0.0032 0.0045 0.0061 0.0081 0.0105

0.0134 0.0165 0.0202 0.0242 0.0286 0.0332 0.0385

0.0437 0.0490 0.0549 0.0608 0.0666 0.0728 0.0787

0.0850 0.0908 0.0969 0.1022 0.1077 0.1134 0.1181

0.1233 0.1279 0.1324 0.1366 0.1404 0.1440 0.1475

0.1505 0.1534 0.1560 0.1582 0.1603 0.1622 0.1639

0.1653 0.1665 0.1676 0.1684 0.1691 0.1695 0.1698

0.1699 0.1701 0.1699 0.1698 0.1693 0.1689 0.1683

0.1678 0.1670 0.1660 0.1653 0.1643 0.1632 0.1623

0.1611 0.1598 0.1587 0.1573 0.1560 0.1547 0.1533

0.1520 0.1506 0.1491 0.1477 0.1462 0.1448 0.1432

0.1417 0.1402 0.1387 0.1372 0.6237 0.1342 0.1327

1.0000 0.1296 0.1281 0.1266 0.1251 0.1237 0.1222

0.1206 0.1192 0.1178 0.1163 0.1148 0.1134 0.1120

0.1105 0.4195 0.1077 0.1063 0.1049 0.1865 0.0981

0.0771 0.0766 0.0759 0.0754 0.0748 0.0742 0.0736

0.0729 0.0723 0.0717 0.0711 0.0704 0.0697 0.0691

0.0684 0.0677 0.0670 0.0663 0.0656 0.0649 0.0641

0.0634 0.0626 0.0619 0.0612 0.0605 0.0597 0.0590

0.0581 0.0574 0.0566 0.0558 0.0551 0.0543 0.0535

0.0527 0.0520 0.0511 0.0503 0.0495 0.0487 0.0479

0.0471 0.0463 0.0455 0.0447 0.0439 0.0430 0.0422

0.0414 0.0406 0.0398 0.0389 0.0381 0.0373 0.0365

0.0356 0.0348 0.0340 0.0331 0.0323 0.0315 0.0307

0.0298 0.0290 0.0282 0.0274 0.0265 0.0257 0.0249

0.0240 0.0232 0.0224 0.0216 0.0208 0.0199 0.0191

0.0183 0.0175 0.0167 0.0159 0.0150 0.0142 0.0134

0.0126 0.0118 0.0110 0.0102 0.0094 0.0086 0.0078

0.0070 0.0062 0.0054 0.0046 0.0039 0.0031 0.0023

0.0015 0.0008 0.0001

5.08E-11 inv sec

C ===== AmBe Neutron Source Energies

SI10 H 1.00e-7 4.14e-7 8.76e-7 1.86e-6 5.04e-6

1.07e-5 3.73e-5 1.01e-4 2.14e-4 4.54e-4

1.58e-3 3.35e-3 7.10e-3 1.50e-2 2.19e-2

```
    2.42e-2   2.61e-2   3.18e-2   4.09e-2   6.74e-2
    1.11e-1   1.83e-1   2.97e-1   3.69e-1   4.98e-1
    6.08e-1   7.43e-1   8.21e-1   1.00      1.35
    1.65      1.92      2.23      2.35      2.37
    2.47      2.73      3.01      3.68      4.97
    6.07      7.41      8.61      1.00e1    1.22e1
    1.42e1    1.73e1
C ===== AmBe Neutron Source Probabilities
SP10    D    0.00      0.00      6.04e-8   1.28e-7   4.16e-7
    7.36e-7   3.47e-6   8.36e-6   1.48e-5   3.13e-5
    1.48e-4   2.30e-4   4.90e-4   1.04e-3   8.93e-4
    3.00e-4   2.46e-4   7.53e-4   1.18e-3   3.46e-3
    5.73e-3   1.09e-2   1.73e-2   1.08e-2   1.92e-2
    1.54e-2   1.80e-2   9.02e-3   2.03e-2   3.37e-2
    2.56e-2   2.55e-2   3.16e-2   1.17e-2   2.00e-3
    1.03e-2   2.93e-2   4.24e-2   1.08e-1   1.81e-1
    1.27e-1   1.11e-1   8.09e-2   3.16e-2   1.22e-2
    0.00      0.00



9.16E-13 inv sec
C ===== PuBe Neutron Source Energies
SI10    H    1.00E-11    1.00E-02      2.00E-02     5.00E-02   1.00E-01
    2.00E-01    4.00E-01     6.00E-01    8.00E-01 1.00E+00
```

```
    1.30E+00    1.70E+00    2.10E+00   2.40E+00   2.70E+00
    3.00E+00    3.30E+00   3.60E+00   4.00E+00    4.40E+00
    5.00E+00    6.00E+00   7.00E+00   8.00E+00   9.00E+00
    1.00E+01   1.20E+01 1.50E+01    2.00E+01
C ===== PuBe Neutron Source Probabilities
SP10    D    0.0    1.47E+00     4.25E+00    2.53E+01   7.62E+01   2.29E+02
    3.81E+03    1.57E+04   2.39E+04   2.59E+04   3.83E+04    3.87E+04
    4.67E+04   4.65E+04   5.67E+04   9.16E+04    1.17E+05   1.10E+05
    1.35E+05    1.23E+05    1.65E+05    1.65E+05   1.53E+05   1.73E+05
    1.30E+05    7.86E+04   1.08E+04   7.41E-02     4.22E-03
```